19 Europa

Christopher F. Chyba
Princeton University
Cynthia B. Phillips
SETI Institute

19.1 Introduction

Europa, one of the four large satellites of Jupiter, is nearly the size of Earth's Moon. Tidal flexing driven by Jupiter's gravity and sustained by an orbital resonance with two other jovian satellites, Io and Ganymede, results in significant heat dissipation within Europa. Calculations indicate that this tidal heating is sufficient to maintain liquid water beneath Europa's ice crust. Moreover, observational evidence suggests that it is indeed probable, but not yet certain, that Europa harbors a subsurface ocean of liquid water whose volume is about twice that of Earth's oceans. The likely presence of abundant liquid water places Europa among the highest priority targets for astrobiology.

To support life, Europa would also require an inventory of biogenic elements and a source of sufficient free energy. The ability to support life does not of course guarantee that the origin of life took place on Europa, or that life is present today; answering these questions will require further exploration. This chapter considers Europa in an astrobiological context, distinguishing among what is known, what is supported by evidence but still uncertain, and what remains more speculative. We conclude with a discussion of the further missions that will be needed to address current geological and astrobiological questions.

19.2 Jupiter and its satellites

The planet Jupiter, orbiting the Sun at 5.2 AU, is more massive than the other planets in the Solar System combined; it is 3.3 times more massive than Saturn and 318 times more than the Earth. Jupiter is a gas giant (Chapter 3), with most of its mass in the form of hydrogen (by number about 86%) and helium (over 13%). Models suggest that it contains a solid core of rock and ice of about 10 Earth masses (Guillot, 1999). Its outer portion (20% by radius) consists of gaseous molecular hydrogen and helium, which we would traditionally call an atmosphere. Beneath this outer gaseous layer, hydrogen is transformed into a liquid metallic state. This phase can only form under extremely high pressures and temperatures, and in our Solar System is thought to exist only in the interiors of Jupiter and Saturn (Stevenson, 1982). Liquid metallic hydrogen is an excellent conductor, and the strong magnetic field of Jupiter is thought to be generated by electrical currents in this layer. The jovian magnetosphere extends out to about 10 Jupiter radii (R_J), between the orbits of Europa (9.4 R_J) and Ganymede (15 R_J). Large numbers of charged particles accelerated in Jupiter's magnetosphere cause problems for probes such as the Galileo spacecraft and would provide a severe challenge to human exploration. This radiation environment also results in interesting chemistry as these particles impact and interact with Europa's surface (Section 19.4). The stunning cloud layers in Jupiter's upper atmosphere are thought to be combinations of ammonia ice, water ice, and small amounts of sulfur, phosphorous, and other compounds that produce bands ranging in color from reds to yellows to whites. The energy that drives Jupiter's strong storm systems and other weather has a substantial internal component; in fact, Jupiter emits $\sim$1.7 times as much energy as it absorbs from the Sun. This excess flux of energy is due to the ongoing loss of heat derived from slow gravitational contraction, a process that has been happening ever since Jupiter formed 4.6 Ga.

Jupiter's four large satellites were discovered by Galileo in 1610 using a small telescope (Galileo, 1610). This discovery of objects orbiting a celestial body other than Earth helped replace the geocentric view of the universe with the heliocentric model, with important religious, philosophical, and scientific consequences. These Galilean satellites (Fig. 19.1) are (in

Planets and Life: the Emerging Science of Astrobiology, eds. Woodruff T. Sullivan, III and John A. Baross. Published by Cambridge University Press.

FIGURE 19.1 Four Galilean satellites. The four large satellites of Jupiter to scale, from left to right: Io, Europa, Ganymede, and Callisto. Io is a volcanic world covered with bright volcanic deposits ranging in color from red to yellow to black to white. Europa's icy surface is covered with linear features and disrupted regions, which appear dark in this global view. The white splotch is an impact crater. Ganymede, the largest satellite in the Solar System, is larger than both Mercury and Pluto, with a surface covered with old tectonic features and bright impact craters. Callisto's surface, the oldest of the Galilean satellites, consists of dark dusty ice covered with bright impact craters of all sizes.

order from Jupiter): Io, a brightly colored, actively volcanic body; Europa, an ice-covered world with a young surface; Ganymede, a rock and ice body with some old cratered areas and some younger terrains; and Callisto, a body with an old surface superficially resembling Earth's heavily cratered Moon. Io and Europa are about the size of Earth's Moon, while Ganymede and Callisto are the size of the planet Mercury. Table 19.1 lists values for various properties of the Galilean satellites.

The Galilean satellites resemble a miniature solar system, and are thought to have condensed out of material orbiting Jupiter in much the same way as the planets condensed 4.6 Ga out of material in the dust and gas disk surrounding the young Sun (Chapter 3). There is a gradation in composition and density from rocky, dense, almost water-free Io (mean density of $3.5\,\mathrm{g\,cm^{-3}}$); to Europa, with an ice/liquid water layer over rock ($3.0\,\mathrm{g\,cm^{-3}}$); to Ganymede, with a thick water ice mantle over a large rock/metal core ($1.9\,\mathrm{g\,cm^{-3}}$); to lowest density Callisto ($1.8\,\mathrm{g\,cm^{-3}}$), which may not be completely differentiated and could have a more uniform mixture of rock and ice. This gradation is reminiscent of the change with distance from the Sun in the volatile content and density of the planets, from metallic and rocky high-density Mercury out to the icy outer Solar System (where, for example, comets are 40–50% water ice by mass). As discussed in Chapter 3, the Solar System's variation in volatile content and density is thought to have come from a temperature gradient in the primordial disk from which the planets condensed; the "snow line," where water could condense, is thought to have been near the orbit of Jupiter, which is why the worlds of the outer Solar System have a much higher volatile content than those closer to the Sun. Similar primordial gradients could explain the Jupiter system as well, but this interpretation is complicated by the possibility that initially present volatiles may have been driven off Io, and perhaps Europa to a lesser extent, by intense geologic activity caused by tidal heating.

19.3 Tidal evolution, resonances, and heating in the Galilean moons

Each of the Galilean moons is *tidally locked* (or "spin-locked") to Jupiter, meaning that it always keeps the same face to Jupiter, that is, it rotates about its pole with a period identical to its orbital period. For Europa this period is 3.6 Earth days (Table 19.1). Such a spin-locked situation (also called *synchronous rotation*) is common among the satellites in our Solar System that orbit close to their primaries[1] (e.g., Earth's Moon always keeps the same face to its primary, Earth), and is due to torques[2] generated by the gravitational force of the primary acting on the tidal bulges raised by the

[1] A *primary* refers to the more massive of two bodies in a mutual orbit about their common center of mass. If the primary body is much more massive than the other body (the satellite), then the center of mass is in fact close to the center of the primary and one often loosely says the satellite is orbiting about the primary.

[2] A *torque* is a change in angular momentum per unit time, and is typically caused by a force acting on an off-axis portion of a body. *Angular momentum* is a measure of a body's rotational (spin) or

TABLE 19.1 The Galilean satellites and Earth's Moon*+

	Io	Europa	Ganymede	Callisto	Earth's Moon
Radius (km)	1822	1561	2631	2410	1738
Mass (10^{21} kg)	89.3	48.0	148.2	107.6	73.5
Mean density (g cm^{-3})	3.53	3.01	1.94	1.83	3.34
Surface gravity (cm s^{-2})	180	131	142	124	162
Escape velocity (km s^{-1})	2.6	2.0	2.7	2.4	2.4
Visual geometric albedo	0.62	0.68	0.44	0.19	0.12
Average surface temperature (K)	118	103	113	118	253
Orbits					
Semimajor axis (R_J)	5.91	9.40	15.0	26.4	5.38 ($=60.1\,R_\oplus$)
Period (days)	1.769	3.551	7.155	16.689	27.322
Eccentricity	0.004	0.0101	0.0015	0.007	0.055
Inclination (deg)	0.04	0.47	0.21	0.51	5.15

Notes:
*Data from National Space Science Data Center (2004).
+Jupiter also has dozens of smaller moons, whose combined mass is about one-thousandth that of Europa.

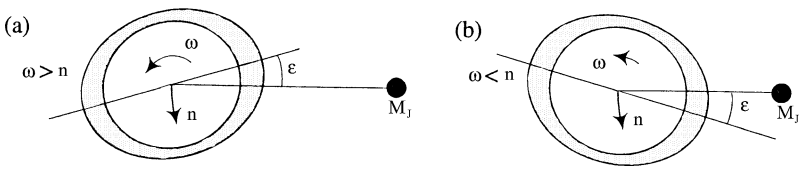

FIGURE 19.2 Tidal bulge and tidal spin-locking. Europa orbits Jupiter (mass M_J) with mean motion n while rotating at angular frequency ω. There is a lag angle ε between the radial line from Europa to Jupiter and the line of symmetry of Europa's tidal bulge. (a) If $\omega > n$, $\varepsilon > 0$ and jovian torques act to decrease ω; or (b) If $\omega < n$, $\varepsilon < 0$ and ω is increased. Drawing is not to scale: Europa's diameter is only 2.2% that of Jupiter, and its orbit is at 9.4 jovian radii. Europa's permanent tidal bulge is also greatly exaggerated.

primary on the satellite.[3] These torques act either (a) to slow the satellite's rotation[4] if its spin angular velocity ω is faster than its mean orbital angular velocity n, or (b) to increase it if $\omega < n$ (Fig. 19.2). When $\omega = n$, torques go to zero for a circular orbit, and a stable state is reached (see Appendix 19.1[5]). Because tidal effects decline rapidly with distance from the primary and also depend on the masses of the primary and the satellite, timescales to reach spin (or orbital) end-states for various objects in the Solar System can vary from geologically short (perhaps as quick as $\sim 10^3$ yr for Europa – see Appendix 19.1) to longer than 10 Gyr.

Tidal evolution also acts to make orbits circular, i.e., to drive satellites' eccentricities e to zero for satellites orbiting close to massive primaries (Appendix 19.2 gives the details). Figure 19.3 explains orbital elements such as *eccentricity* and *semimajor axis*. The timescale for orbit circularization is longer than the despinning timescale because satellite spin angular momenta are typically very small in comparison to their orbital angular momenta.

Jupiter's strong gravity raises tidal bulges along the line towards Jupiter (Appendix 19.1 and Fig. 19.2), but

orbital momentum, and, like linear momentum, is a quantity that in general is conserved.

[3] The gravitational force between two bodies is proportional to the product of their masses divided by the distance squared between the bodies. A *tidal force* refers to the *difference* between the gravitational force of an external body acting on one side of a body (say the near side) to that acting on another side (say the far side). Tides due to an external body create symmetric distortions (bulges) in a second body of an amplitude proportional to the inverse *cube* of their separation.

[4] This process is called *despinning* and is the more common situation.

[5] The appendices at the end of this chapter present greater detail about the physics of the Jupiter–Europa system; they may be skipped without loss of continuity.

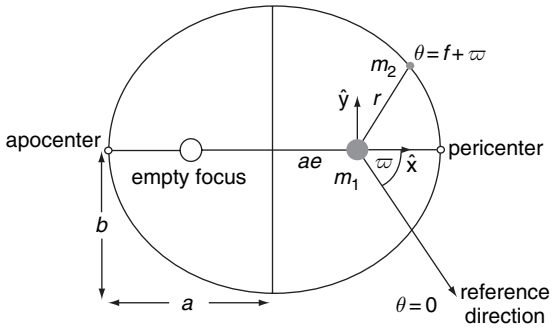

FIGURE 19.3 Orbital elements. Standard notation used to describe a Keplerian orbit of semi-major axis *a*, semi-minor axis *b*, and eccentricity e. *Pericenter* and *apocenter* are the minimum and maximum distance of the satellite m_2 from the primary body m_1. The eccentricity e of the orbit, a measure of its deviation from a circle ($e = 0$) is defined as $e = \sqrt{(1 - b^2/a^2)}$. The longitude of pericenter $\bar{\omega}$(measures the angular position of the pericenter from a chosen reference direction. (After Murray and Dermott, 2001).

since the distance to Jupiter varies for any satellite with a non-circular orbit, Jupiter's gravitational force and thus the tidal bulge's height also vary around the satellite's orbit. The satellite's figure is flexed as the bulge moves up and down, producing an internal dissipation of energy called *tidal heating* (Appendix 19.3 contains details). Since the satellite's orbit is eccentric, its orbital velocity also varies around its orbit (faster when closer), so that its spin-locked *constant* rate of rotation does not keep perfect pace with its *variable* orbital velocity. The result is a slight "sloshing" or *libration* of the satellite's tidal bulge back and forth around the radial line to Jupiter. This libration tide also contributes substantially to the tidal heating of the satellite (Appendix 19.3). Energy dissipation (tidal heating) from both these tidal effects acts to circularize the satellite's orbit.

Once any satellite is both spin-locked and driven into a circular orbit, its tidal bulge will no longer vary around the orbit and tidal heating will cease. However, despite tidal dissipation and the resulting tendency toward orbital circularization, the orbits of the inner Galilean satellites are all slightly non-circular (Table 19.1). These "forced" eccentricities are maintained by the satellites' mutual periodic perturbations in a so-called *Laplace resonance* (Fig. 19.4), first shown by and then named after the French mathematician and physicist (1749–1827).

Io, Europa, and Ganymede are in a 1:2:4 *orbital resonance*, meaning that Ganymede's orbital period is very nearly twice that of Europa's, which is very nearly twice that of Io's. This resonance is *stable*, meaning

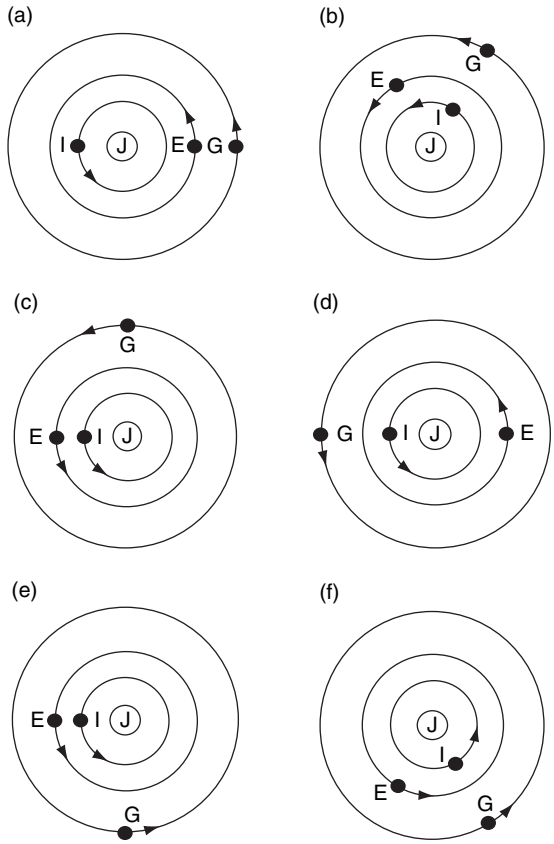

FIGURE 19.4 The Laplace resonance. (a) through (f) show the sequence of conjunctions for the three Galilean satellites (I = Io, E = Europa, G = Ganymede) that participate in the resonance as they orbit about Jupiter (J). The seventh configuration in the sequence would complete one period of Ganymede (which is two periods of Europa and four periods of Io) and return to (a). (Murray and Dermott, 2001).

that the effects of any perturbations to the situation (say, caused by the gravity of a passing planet or of the moons themselves) will eventually die out and the system will remain unchanged. The configuration of the Galilean system is such that whenever two of the three inner satellites are in conjunction, the third is at least 60° away as seen from Jupiter (Fig. 19.4). Because Io and Europa, or Europa and Ganymede, line up periodically at the same points in their orbits, each pair experiences regular gravitational perturbations that do not average out over many orbits. These perturbations maintain the forced eccentricities of the satellites' orbits and thus sustain tidal heating over time. Appendix 19.4 gives the details of how the Laplace resonance works.

Since tidal heating is driven by Jupiter's gravity, which falls off like the square of the distance, the tidal

heating is most intense at the innermost moon Io. Io is in fact the most volcanically active body in the Solar System, surpassing even the Earth. Io's volcanic activity was brilliantly predicted by Peale, Cassen, and Reynolds (1979) in a paper published three weeks prior to the Voyager 1 spacecraft's arrival at the jovian system. If the current rate of volcanic activity on Io is typical over its history, then there has been sufficient volcanic processing to recycle the entire crust of Io out onto the surface many times. This activity may well have driven off most volatiles over time – indeed any water present on Io at its formation would now be long gone.

Europa is farther away from Jupiter than Io (9.4 vs. 5.9 R_J), so despite its orbit's larger eccentricity (0.010 vs. 0.004) it experiences less tidal heating, which depends on eccentricity e and semimajor axis a like $e^2a^{-15/2}$ (Appendix 19.3, Eq. (19.8)). Nevertheless, a substantial amount of heat is dissipated within Europa's core, mantle, and ice shell, although there is an ongoing debate over exactly how much is dissipated overall and within each layer (Appendix 19.3).

More distant Ganymede at 15 R_J is also subject to tidal heating, though less so. Still, Ganymede may have experienced sufficient tidal heating to drive some geologic activity and internally differentiate into an icy mantle and a rock/metal core. Ganymede's surface includes old, cratered terrain, but also younger grooved and ridged areas which are the result of more recent tectonic activity. An interesting comparison can be made between Ganymede and its neighboring satellite Callisto, which is nearly the same size as Ganymede. Callisto does not participate in the resonance with the other three Galilean satellites, and is an old, cratered body with few, if any, signs of geologic activity. Callisto also is thought not to be fully differentiated, although recent measurements suggest that it could have a small core.

19.4 Europa's space environment

Europa orbits Jupiter at a distance of 9.4 Jupiter radii (671,000 km) with an orbital period of 3.55 days, and has a diameter of 1560 km (just under the size of Earth's Moon). Its *albedo* is ~0.68, meaning that it reflects 68% of the visual sunlight incident on it, making it one of the brighter objects in the Solar System (for comparison, Earth's Moon's albedo is 0.12). Note that most of the publicly released images of Europa are considerably contrast-enhanced, and that the difference in brightness between the bright and dark regions of Europa's surface is actually small. Europa's surface temperature has been measured to be as high as 130 K at the equator in daytime (Spencer *et al*., 1999) and could drop as low as 50 K at the poles.

19.4.1 UV and charged particle bombardment

Europa's charged particle and ultraviolet (UV) radiation environment has been measured by the Galileo spacecraft and is summarized in detail by Cooper *et al*., (2001). The solar irradiation of its surface is smaller than that at Earth's distance from the Sun by a factor $(5.2)^2 \approx 27$ and totals 8×10^{12} keV cm^{-2} sec^{-1}; the incident ultraviolet-C (UV-C) flux[6] ($\lambda < 280$ nm) is 4×10^{10} keV cm^{-2} sec^{-1}.

Europa's harsh charged-particle radiation environmet is due primarily to the acceleration of these particles in Jupiter's magnetosphere. The incident energy flux of charged particles is $\sim 8 \times 10^{10}$ keV cm^{-2} sec^{-1}, about twice that due to UV-C. It is dominated by energetic electrons in the keV to MeV range, but includes H^+, O^{n+}, and S^{n+} ions as well. The depths affected by this radiation depend on the density of the surface, which could range from that for solid ice (0.92 g cm^{-3}) to that for water frost (~0.1 g cm^{-3}). Since the density of Europa's uppermost surface is unknown, penetration depths are given in terms of mass cross sections; the average stopping depth for the most penetrating charged particles, the electrons, is 0.62 g cm^{-2}, corresponding to a depth of ~0.7 mm in 0.92 g cm^{-3} ice. These depths are much greater than those penetrated by UV photons, which affect only the top sub-micrometer layer; for example, Lyman-α photons ($\lambda = 121.6$ nm) have a mean penetration depth of only 0.04 μm in ice.

A crude understanding of the implications of the incident radiation fluxes cited above for materials or biology can be obtained by calculating net volume radiation dose rates as a function of depth into Europa's ice (Fig. 19.5). Depths of 1 cm in Europa's ice (assuming an ice density of 1 g cm^{-3}) experience a volume dosage rate of ~ 0.3 Mrad per month (Cooper *et al*., 2001). This dose is hundreds of times higher than the lethal dose for human beings (a lethal dose for 50% of humans is ~0.0006 Mrad). The most radiation-resistant terrestrial organism known, *Deinococcus radiodurans*, has 90% survival after 6 Mrad, dropping to 10^{-6} survival after 12 Mrad of ionizing radiation

[6] Energies greater than ~4.4 eV, corresponding to photon wavelengths below 280 nm, are required to dissociate H_2O, so UV-C fluxes are those of relevance to radiation chemistry.

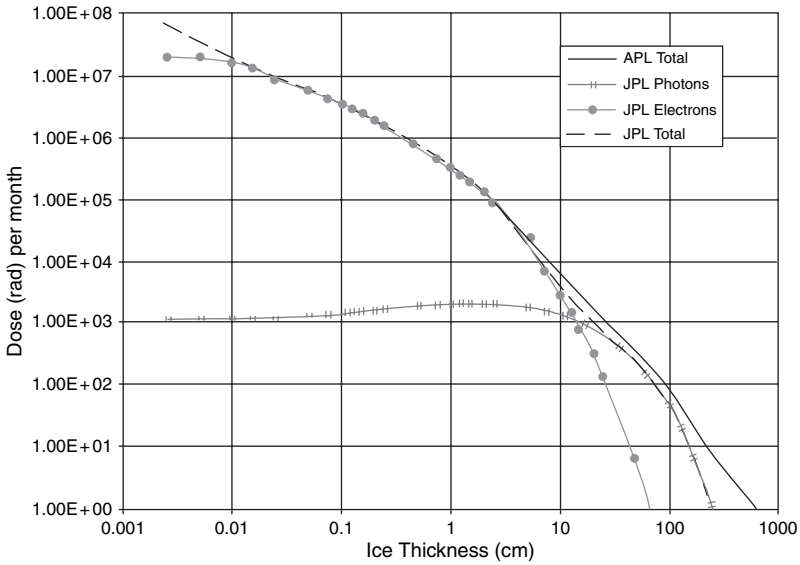

FIGURE 19.5 Radiation dose in ice. The dose in units of rad (water) per month (30.4 days) of exposure beneath a given thickness of ice for both UV photons and electrons. Information provided by researchers at the Jet Propulsion Laboratory (JPL) and the Applied Physics Laboratory (APL). (After Space Studies Board, 2000).

dose (Auda and Emborg, 1973). Radiation doses fall rapidly with depth in Europa's ice, so that at meter depths monthly doses are ~100 rad; doses drop to values similar to those in Earth's biosphere at depths of 20 to 40 m. An ocean beneath kilometers of ice would be entirely protected; microorganisms living in putative near-surface niches of liquid water, especially if these were close enough to the surface to permit photosynthesis (Greenberg *et al.*, 2000), would have to cope with the resulting radiation stress. This alone does not seem insurmountable for highly resistant strains; *D. radiodurans* could survive at the 90% level for nearly two years at 1 cm depth in Europa's ice. Using terrestrial algal mats growing on the bottoms of permanently ice-covered Antarctic lakes as an analogue, it appears that photosynthesis should be possible beneath ice thicknesses of ~15 m on Europa (Reynolds *et al.*, 1983), where the radiation dose would be tolerable by many organisms. More recent work by Warren *et al.* (2002) suggests that photosynthesis is possible at light levels lower than those considered by Reynolds *et al.* (1983), implying that photosynthesis could be possible under a few tens of meters of europan ice. If near-surface liquid water niches do in fact exist, microbial photosynthesis on Europa would seem possible.

19.4.2 Sputtering

Sputtering is erosion of a surface by charged particle impacts. Sputtering at these high energies is explosive – many thousands of water molecules are removed from the surface for each single incident high-energy ion. The best estimate for the sputtering erosion rate on Europa due to energetic H^+, O^{n+}, and S^{n+} ions is about $0.02\,\mu m\,yr^{-1}$ for erosion of surface molecules of H_2O (Cooper *et al.*, 2001), although some previous estimates have been as much as 100 times higher. Over Europa's ~50 Myr surface age (Section 19.4.3), sputtering thus should have removed ~1 m of material.

Europa's tenuous atmosphere, due mostly to oxygen sputtered from its surface ice, is in fact a near-vacuum with a surface number density of O_2 gas of $\sim 10^8$–$10^9\,cm^{-3}$ (Ip, 1996), equivalent to that at ~400 km altitude in Earth's atmosphere. Atomic sodium is also present in Europa's atmosphere and could come either from a source such as material ejected volcanically from Io, or perhaps from an europan source.

19.4.3 Impacts and gardening

Europa, like all other Solar System bodies, is subject to impacts by comets, asteroids, and smaller objects. Gravitational focusing (Section 3.9.2) by Jupiter's large mass enhances the impact flux experienced by Europa. The main objects impacting Europa and the other bodies in the jovian system are thought to be Jupiter family comets (Zahnle *et al.*, 1998), of which a spectacular example was the impact of comet Shoemaker–Levy 9 with Jupiter in 1994. Shoemaker–Levy 9 was gravitationally disrupted into multiple pieces during an earlier pass by Jupiter, and then impacted Jupiter in a series of well-documented collisions.

The number of craters on planets and satellites can be used to gauge both relative and, with additional information, absolute surface ages. Europa's surface has only about 15 impact craters with diameters greater than 10 km (Moore *et al.*, 2001), and the majority of small craters seem to be secondary craters formed by debris thrown out from these large events. This lack of craters implies a young surface, because recent (or perhaps current) geologic activity is required to erase them. Bodies with current geologic activity such as Io and Earth have very few recognizable impact craters – Io, in fact, is so volcanically active that not a single impact crater, of any size, has been found on its surface to date! The Earth has about 150 recognized craters, but many have been geologically modified and would be difficult to recognize from orbit. On the other hand, geologically inactive bodies with old surfaces such as Earth's Moon or Callisto are covered with impact craters of all sizes. The most densely cratered surfaces are said to be "saturated", as each new crater destroys old craters beneath it.

Relative ages can be deduced by comparing the number density of craters on different parts of a planet or satellite's surface. Europa's crater density is so low, however, that no part of the surface has been reliably inferred to be younger or older than any other. With respect to absolute age, various efforts have been made to establish impact fluxes throughout the Solar System's history in order to establish the actual age of a body's surface based on its crater density. From calculations of the comet and asteroid fluxes at Jupiter, the age of Europa's surface has been estimated to be only ~50 Myr. Despite Europa's geologically young surface (by comparison, the majority of Earth's surface, the ocean floors, are typically 100–200 Myr in age), no current geologic activity was found to a resolution of ~2 km over 20% of Europa's surface in a comparison between Voyager and Galileo spacecraft images taken 20 years apart (Phillips *et al.*, 2000).

Europa's surface is subject to a range of impacts extending in size from those responsible for the largest observed craters down to micrometeorites. These impacts together result in the formation of a *regolith*, a layer of broken impact debris at the surface of an airless world that is continually mixed through a process called *impact gardening*. The depth to which surface material has been mixed after a given length of time is called the gardening depth. Impact gardening can potentially preserve surface material by moving it down below the sputtering depth and even the effective radiation penetration depth. If sputtering dominates, compounds produced by radiation processing at the surface are lost before they have a chance to be buried and possibly eventually transported to a subsurface ocean layer (Section 19.10.4). However, if gardening dominates, then material may be buried faster than most of it can be removed through sputtering.

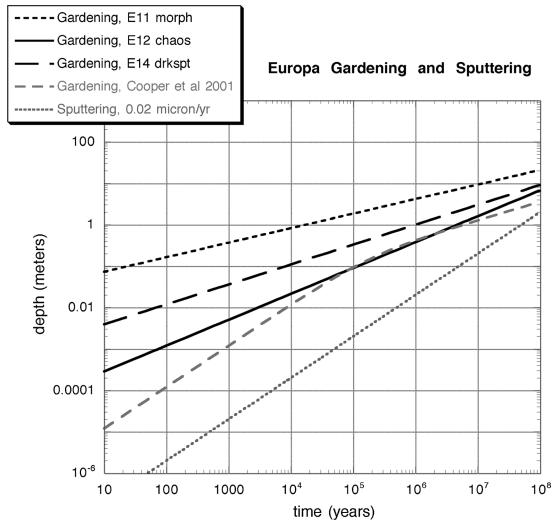

FIGURE 19.6 Impact gardening on Europa. Three estimates of gardening rates, labeled E11, E12, and E14 for different regions of the surface imaged on separate Galileo flybys of Europa, are compared with a previous gardening rate (Cooper *et al.*, 2001) and the sputtering rate. Note that all these gardening rates dominate over sputtering over the presumed age of Europa's surface.

Models for gardening on Europa remain poorly developed. Cooper *et al.* (2001) scaled from Ganymede regolith depth estimates, as well as a mass flux from studies of rings, to estimate a gardening depth of 2.6 m over a surface age of 50 Myr. The present authors have found a similar result using a model of impact gardening based on studies of the lunar regolith coupled with estimates of the impactor population in the outer Solar System (Zahnle *et al.*, 1998). Further refinement of the models, taking into account studies of the numbers of very small craters on Europa, indicates that the gardening depth could extend deeper than earlier estimates, and that depths of 1–10 m per 10 Myr could be achieved (Fig. 19.6). For a sputtering erosion rate of $0.02\,\mu m\,yr^{-1}$, any of the gardening estimates so far discussed suggests that gardening dominates sputtering by an order of magnitude over Europa's surface age.

19.5 Surface composition

We have no samples of Europa's surface nor any results from *in situ* measurements, so spectroscopy, which

samples only the top few microns of the surface, is currently our only source of precise information regarding Europa's surface composition. Even before the Voyager spacecraft arrived at Jupiter in 1979, ground-based spectroscopy had shown that Europa's surface was predominantly water ice. The Galileo spacecraft's near-infrared spectrometer detected absorption features on Europa due to sulfur dioxide (SO_2) and hydrogen peroxide (H_2O_2; present at 0.13% by number relative to H_2O). Oxidants such as H_2O_2 and O_2 at Europa's surface are an expected product of charged-particle bombardment of water ice (Delitsky and Lane, 1998) and have important astrobiological implications (Section 19.11).

Observed near-infrared ice absorption bands (from 1.0 to 2.0 μm) show distortions from those for pure water; these distortions have been modeled as due to the presence of hydrated salts or other compounds, for example, magnesium sulfate hydrates (e.g., $MgSO_4 \bullet nH_2O$) or bloedite ($Na_2Mg(SO_4)_2 \bullet 4H_2O$) (McCord *et al*., 1999), or sulfuric acid ($H_2SO_4 \bullet 8H_2O$) (Carlson *et al*., 1999a). Hydrated salts in which Na and Mg are the dominant cations and sulfate (SO_4) the dominant anion are consistent with experimental and theoretical studies (Kargel *et al*., 2000, Zolotov and Shock, 2001; but see McKinnon and Zolensky, 2003) that assume evolution from an initial carbonaceous chondrite composition (Chapter 3). The locations of these potential salts are mostly along ridges, in craters, or in the matrix of chaotic terrain (see Section 19.7 for descriptions of Europa's surface features). The composition of the inferred salts is similar from place to place on Europa, consistent with an origin from a globally mixed reservoir. One intriguing explanation for such a reservoir is a global salty water ocean, which reaches the surface in places of recent geologic activity and leaves salts behind. Even the presence of such salts, however, does not unambiguously require a global ocean.

Carbonaceous chondrite meteorites are typically several percent organic by mass, so it is reasonable to expect such compounds on Europa – though an analogy should not be mistaken for evidence. A variety of organic functional groups have been detected on Ganymede and Callisto (such as C≡N and C-H) and there are very low signal-to-noise observations of such compounds on Europa (McCord *et al*., 1998). Carbon dioxide has been observed on Ganymede, Callisto, and Europa; the CO_2 abundance of Europa appears to be about 0.2% by weight (McCord *et al*., 1998). Charged particle irradiation of CO_2-containing H_2O ice should lead to the production of simple organics such as formaldehyde (H_2CO) (Section 19.10).

Dalton *et al*. (2003) have shown that the distortion in the near-infrared ice absorption bands can be fit at least as well by the spectra of 100 K ice and bacteria mixtures as by bloedite, magnesium hexahydrites, or sulfuric acid. That is, to the extent that the spectral features provide evidence for the presence of certain salts present in Europa's ice, these features also provide evidence for europan microorganisms. Dalton's intriguing work provides an important caution about the interpretation of features at low spectral resolution such as that of the Galileo instrument ($\lambda/\Delta\lambda \approx 100$ from 0.7 μm to 5.2 μm). At these low resolutions, features are ambiguous and at risk of misinterpretation.

This is not a new lesson. A similar challenge was experienced with low-resolution near-infrared observations of comet Halley around the time of the Giotto and Vega spacecraft flybys in 1986. A broad spectral feature around 3.4 μm observed with resolution $\lambda/\Delta\lambda \approx 400$ was consistent with emission from an organic grain model based on tholins synthesized in laboratory ice irradiation experiments (Chyba and Sagan, 1987). However, these same features could also be fit by the spectral characteristics of grains rich in bacteria and viruses (Hoyle and Wickramasinghe, 1987). In the end it took 25 times higher resolution to largely resolve these ambiguities. It was ultimately demonstrated that the majority (though not all) of the 3.4 μm feature was due not to organic grains, but to molecular lines of individual organic molecules (such as methanol, CH_3OH) that could not be individually resolved at the lower resolution (Mumma *et al*., 1993). Higher resolution spectra of Europa's surface may likewise be essential to finding the right interpretation of the near-infrared features.

19.6 Interior models

Europa's bulk density of 3.0 g cm^{-3} is substantially lower than that of ice-free Io (Table 19.1). As noted above, spectroscopy by itself only establishes the presence of a thin layer of water ice at Europa's surface, so such observations supported models of a Europa with substantial water ice below its surface, but did not require it.

Voyager images showed an absence of both very dark terrain and substantial topographic relief, suggesting that Europa was covered with at least several km of H_2O, concealing any underlying silicate topography. (Ice that is sufficiently thick and warm beneath the surface cannot support substantial topography because it will deform and flatten over geological timescales; this

is called viscous relaxation (Thomas and Schubert, 1986).) Early thermal models using conductive cooling and heating from radioactive elements predicted the possibility of a differentiated Europa with water ice overlying a silicate/metal core; in this case a Europa whose silicate/metal interior had the same average density as Io ($3.5\,g\,cm^{-3}$) required a surface H_2O layer 120 km thick (Cassen *et al*., 1982), a model that would later be shown by Galileo spacecraft measurements to be broadly correct (see below).

These early models also predicted the possibility of a *liquid* water layer beneath Europa's frozen ice crust. There could be a balance between tidal and radioactive heating, and conductive and convective cooling that would allow a portion of the subsurface water layer to remain liquid over geologic time. Current models have failed to resolve this issue completely (Ojakangas and Stevenson, 1989; McKinnon, 1999), mostly because the properties of ice are poorly known at the temperature of Europa and on the days-long timescales associated with tidal flexing. Also poorly known is the composition of Europa's ice; the addition of small amounts of other volatiles such as ammonia or salts could dramatically change its viscosity (McCord *et al*., 1999). Also important is the physical state of the ice, including its grain size and degree of fracturing, which could affect its strength.

In conclusion, *theoretical* models of tidal heating and deformation suggest that a liquid water layer of thickness up to ~100 km could have been or may currently be present beneath Europa's surface, but cannot definitively say so. In the following sections, however, we present Galileo Mission measurements that further strongly support this view.

19.6.1 Gravity measurements

Radio data from the Galileo spacecraft's close flybys of Europa suggest that Europa is completely *differentiated* (separated into a dense core with less dense overlying layers). This technique uses measurements of the spacecraft's trajectory (via observing the Doppler shifting of its radio signals) to probe the moon's gravity field. Newton (1686) showed in his *Principia*[7] that a perfectly spherical distribution of mass has a gravitational field identical to that of a point of the same mass, i.e., one that falls off like the square of the distance. However, deviations of a body from sphericity (e.g., the oblateness that arises on any spinning world) leads to higher-order terms (terms falling off at powers higher than the square of the distance) in the expression describing its gravitational field. The size of these terms depends on the internal distribution of matter within the body (Appendix 19.5 gives further details). Sufficiently accurate tracking of a spacecraft's trajectory can determine its deviation from that expected for a perfect sphere, and thereby determine the coefficients of some of the higher-order terms in the gravitational field. These in turn give information about the interior mass distribution of the object.

Such measurements from the Galileo spacecraft, combined with our knowledge of Europa's bulk density and the cosmic abundances in the Solar System (Chapter 3) indicate that Europa's most likely internal configuration includes an Fe or Fe-S central core, an anhydrous (lacking water) rocky mantle, and a surface layer of material with a density of around $1\,g\,cm^{-3}$ that is ~100 km thick (with uncertainties ranging from 80 to170 km) (Anderson *et al*., 1998). The only cosmochemically plausible material with this abundance and density is H_2O. Many objects in the outer Solar System are extremely water-rich; comets, for example, are as much as 40–50% water ice by mass. On this interpretation Europa is ~6% H_2O by mass, consistent with the water inventory of a carbonaceous chondrite meteorite. But the gravity data cannot distinguish between liquid water and solid ice due to their nearly identical densities. If this water were predominantly liquid, its volume would be more than double that of all of Earth's oceans. The pressure at the bottom of this ocean would be around twice that in the deepest parts of Earth's oceans.

If the H_2O layer were instead ice all the way down, the most likely interior temperature profiles (Section 19.8) suggest that the ice would be ice I to the bottom.[8] Pressures at the bottom of the thickest H_2O layer (170 km) consistent with the gravity data are ~200 MPa, making ice III a possibility for warm ice at this depth. At lower pressures, unlikely but not impossible conditions of temperature and pressure would permit ice II to exist.

19.6.2 Magnetic field measurements

Perhaps the most convincing evidence for an ocean of liquid water beneath Europa's surface comes from magnetic field measurements. Data from Galileo's magnetometer (Kivelson *et al*., 2000) show that Europa has an

[7] Book I, Sec. XII, Prop. LXXIV, Th. XXXIV.

[8] Section 15.2 gives a phase diagram for H_2O and includes a discussion of the various types of ice (I, II, III, etc.).

induced magnetic field that varies in direction and strength in response to Jupiter's rotating magnetic field. This results from Faraday's law of induction: time variations in a magnetic field cause (induce) an electric field, which (if a conducting material is present) in turn causes (so-called eddy) currents, which in turn create a secondary magnetic field that tends to oppose the original magnetic field (further details are in Appendix 19.6). The periodic variation in direction shows that the field is not due to a permanent internal dipole, i.e., it is not analogous to the Earth's internal field. The strength and response of the induced field at Europa require a near-surface, global, electrically conducting layer.

Similar magnetometer data suggest that Callisto and Ganymede (Kivelson *et al.*, 2002) may also harbor subsurface oceans. These latter oceans may exist in a layer sandwiched between two phases of water ice; if so they would not provide the astrobiologically more interesting rock/water interface (with possibilities for hydrothermal vents, see Section 19.10.3) that may be present at the bottom of Europa's ocean (McCollom, 1999).

The magnetic data for Europa cannot be explained by localized pockets of salty water, and require a nearly complete spherical shell. The induced field cannot be the result of a frozen ice layer, even if it had pockets of briny water, since ions in solid ice would be insufficiently mobile (Stevenson, 2000a). It is possible that a type of conducting layer other than a global salty ocean could account for the induced magnetic field, but the salty ocean explanation is the most plausible. Postulating currents induced in a metallic core does not work because the induced dipole field strength falls off with the cube of the distance and the core is simply too far away to provide the observed field. Nor are the data consistent with a field induced in Europa's ionosphere, which is too tenuous to support the electrical currents needed to explain the field strength (Zimmer *et al.*, 2000).

In addition to the (variable) eddy currents induced in Europa's ocean due to Jupiter's time-varying magnetic field, a *constant* electrical current might also flow because of Europa's orbital motion through the near-constant vertical component of Jupiter's magnetic field. This is due to the Lorentz force $\boldsymbol{F} = q\mathbf{v} \times \boldsymbol{B}$ experienced by a particle of charge q moving with a velocity $\boldsymbol{v}$ relative to a magnetic field $\boldsymbol{B}$.The resulting motion of charge should lead to currents in Europa's ocean that run from Europa's subjovian hemisphere to the antijovian hemisphere. However, these currents are strongly limited by the electrically insulating water ice overlying the ocean (Reynolds *et al.*, 1983; Colburn and Reynolds, 1985). Such electrical currents in Europa's ocean could be considerably greater than those suggested by Colburn and Reynolds (1985) because Europa's ice is expected to be salty, and therefore much more conducting than pure water ice.

19.7 Europan geology

Images of Europa returned by the Voyager spacecraft in 1979 revealed a bright, icy world covered with long linear features, some of which seemed to circle nearly the entire globe. There was also a striking absence of impact craters, suggesting a young surface age. The surface was remarkably smooth, with little topography more than a few hundred meters high. Also visible in the Voyager images (limited by a maximum resolution of ~2 km/pixel) was so-called "mottled terrain," fuzzy-looking dark patches that interrupted the dark linear features and bright background regions. Galileo spacecraft imagery over 1996–2002 revealed many more details of Europa's geology (e.g., Fig. 19.1). About 10% of Europa's surface was imaged at resolutions of 200 m/pixel or higher with very limited coverage at resolutions as high as ~6–10 m/pixel (Greeley *et al.*, 2000). The mottled terrain turns out to consist of areas of disrupted surface, in some cases broken up into coherent iceberg-like blocks that seem to have "rafted" into new positions (Greenberg *et al.*, 1999). Such areas can be reconstructed by fitting the pre-existing features on the blocks back together (Spaun *et al.*, 1998). It is still the case that few large impact craters have been found and the largest impact craters are anomalously shallow (Moore *et al.*, 1998). The topography remains quite low, with just a handful of instances of features over a few hundred meters in height (Greeley *et al.*, 2000). Other features of interest on Europa's surface include regions that could possibly be due to surface flows of low-viscosity material such as liquid water.

Because our interest in this chapter is focused on astrobiology, we survey Europa's geology from the point of view of its implications for the existence of a subsurface ocean (Pappalardo *et al.*, 1999), other pockets of liquid water, and possible communication between Europa's surface and the ocean. Although many models have been proposed for formation of the surface features (see Greeley *et al.* (2004) for a review), virtually all of them take the existence of a subsurface liquid water layer as a starting assumption. The main debate now is over the *thickness* of the overlying ice layer. The thickness of this crust is of interest

for astrobiology, but not crucial to prospects for the existence of subsurface life. Thick- and thin-ice models do affect, however, proposed mechanisms for providing speculative europan biospheres with the free energy they would need to persist (Section 19.10). A thin crust would also make direct exploration of the liquid layer easier for future spacecraft (although still extremely challenging). Lastly, if life does exist in the liquid layer, a thin-ice cover would seem to allow remnants to be more readily found at the surface.

19.7.1 Lineaments

The dominant surface features on Europa are linear ridges and bands called *lineaments*. Of these, *ridges* are long linear features usually a kilometer or so wide, a few hundred meters tall, and hundreds or thousands of kilometers long. The common "double ridge" (Fig. 19.7) has two symmetrical ridges separated by a central trough. *Bands*, by contrast, consist of multiple parallel linear features with little or no topographic expression. Their formation may or may not be similar to the formation of ridges. There is also a background terrain of many small ridges and cracks, with a variety of orientations.

Most models of ridge formation begin with a crack generated through tidal flexing (Hoppa *et al.*,1999a), and various mechanisms then exploit this zone of weakness to create a ridge. Models vary in requirements for ice thickness, ranging from a very thin crust overlying liquid water to completely solid-state models with a thin, brittle crust on top of a lower-viscosity, warm ice layer.

The tidal squeezing model proposed by Greenberg *et al.* (1998) assumes a thin ice layer overlying liquid water, and relies on diurnal tides to open and close a crack. Whenever the crack is open, water or slush enters the crack, and this material is then squeezed up to the surface when the crack closes again half a period later. Over time, this material is built up on both sides of the crack, producing the signature double ridge frequently seen on Europa.

The thick ice models of ridge formation again start with a tidal crack at the surface. An upwelling linear *diapir* (a buoyant plume of warmer, soft ice) then rises to exploit this zone of weakness, and warps the overlying crust when it nears the surface (Head *et al.*, 1999). This mechanism explains the observation that preexisting features are sometimes visible on the upwarped ridge flanks, suggesting that the entire surface has been lifted rather than covered with material in a depositional mechanism such as in the tidal squeezing model. (See the upper right-hand corner of Fig. 19.7 for an example.) The linear diapir model requires that solid state convection is taking place in a thick warm ice crust which may or may not overlie a liquid ocean layer. It also requires, for solid state convection to begin, that the ice layer has a thin brittle shell at the surface, and a warmer, lower-viscosity layer of at least 10 km thickness (McKinnon, 1999). There are other suggested ridge-formation mechanisms, including a *cryovolcanism*[9] model in which material is explosively vented onto the surface, building up ridge margins surrounding a crack (Fagents *et al.*, 2000).

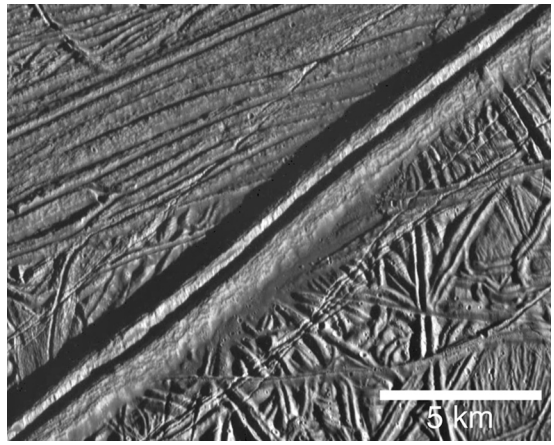

FIGURE 19.7 A ridge. The predominant ridge type on Europa is double, consisting of parallel ridges symmetrical about a central trough. Double ridges are usually ~1 km wide, a few hundred meters tall, and can stretch for hundreds or thousands of km in length. The pictured ridge is superimposed on a background plain of older, smaller ridges.

A different and striking ridge type on Europa is the *cycloidal ridge* (Fig. 19.8). These appear as a series of connected arcs that march across the surface like a child's drawing of waves on an ocean. In an elegant model of global tidal stress orientations and magnitudes, cycloidal ridges have been shown to correspond in orientation and location to cracking of the surface in response to changing diurnal tidal stresses (Hoppa *et al.*, 1999b). In some cases this model predicts that cracks on the surface propagate at a speed of $\sim 3\,\mathrm{km\,hr^{-1}}$, a good walking pace! This model requires the existence of a global ocean to obtain a large enough, time-varying tidal bulge to give sufficient tidal stresses

[9] *Cryovolcanism* refers to ice volcanism, specifically the eruption of liquid or vapour phases of water or other volatiles that would be frozen at the normal temperature of the icy satellite's surface (Geissler, 2000).

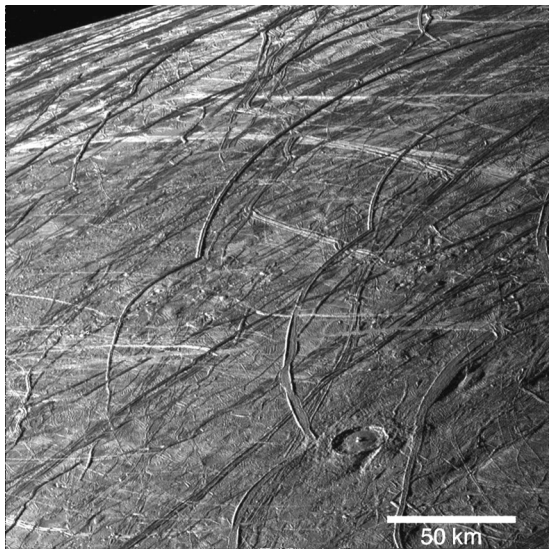

FIGURE 19.8 Cycloids and a large crater. Cycloidal ridges are thought to be formed by the changing orientation of tidal stresses during Europa's 3.6-day orbit around Jupiter. Such ridges are more often found at high northern and southern latitudes, and contain many arcs and cusps of varying sizes and orientations. The 20-km diameter crater in this image is Maeve (58° N, 75° W), and illustrates the shallow appearance of impact craters on Europa's surface.

to crack the ice. The cycloidal ridge model explains the shapes of the cracks, but does not determine how the ridge is built up once the crack exists.

It is unclear whether any of the proposed ridge formation models can explain how some ridges maintain such a uniform, linear appearance over thousands of kilometers. Clearly, the various proposed models are contradictory, and have very different implications for Europa's subsurface structure and the location or existence of a subsurface water layer. These questions and contradictions emphasize the need for a future mission to Europa.

19.7.2 Bands

Bands on Europa are similar to ridges, but clearly represent places where the surface has opened up and been pulled apart, resulting in the extrusion of new surface material in between the older pieces of crust (Fig. 19.9). Bands can be wedge-shaped or long, parallel sets of small ridges and grooves. Reconstructions of pre-existing features cross-cut by the bands show that the bands open along a fracture and then offset, rather than cover over, nearby features (Sullivan *et al.*, 1998). Such pull-apart bands demonstrate that the surface layer has broken and moved; strike-slip motion has also been observed along bands (Tufts *et al.*, 1999). Such motion requires a brittle surface layer on top of a more ductile, lower-viscosity layer. Bands seem to be similar to mid-ocean ridge morphology on Earth (Prockter *et al.*, 2002), and in some cases seem to originate along a pre-existing double ridge that was then pulled apart laterally rather than continuing to grow vertically like a typical ridge. Models exist for their formation in either a thin-ice or thick-ice regime.

An open question has been that if bands and perhaps also ridges are formed by extension, where is the accompanying compression that must be accommodated by Europa's surface? An answer may come from observations of folds detected at Astypalaea Linea (Prockter and Pappalardo, 2000), which suggest that bands could account for both extension and compression in a crustal recycling process on Europa. In this model, bands are formed through spreading of the crust as a large crack opens and pulls apart and new material fills in the gap. However, once a large band forms, it becomes an area of relatively thin, ductile ice which is weaker than the surrounding regions of colder, thicker, firmer ice. It therefore becomes a "target" for global compressional stresses that serve to fold the entire region. Over time, the large-scale topography created by this folding relaxes away, leaving only smaller-scale remnants.

19.7.3 Chaotic terrain and lenticulae

Chaotic terrain, with its resemblance to terrestrial iceberg-like blocks floating in water (Fig. 19.10), would seem to provide good evidence for the presence of liquid water beneath Europa's surface (Greenberg *et al.*, 1999), although other models have been proposed which could form disrupted areas through solid-state ice diapirism (Pappalardo *et al.*, 1998; Sotin *et al.*, 2002). Regions of chaotic terrain are seen as areas of localized heat flow in a thin-crust scenario where the ice layer melted all the way to the surface (crustal thickness temporarily goes to zero) (Greenberg *et al.*, 1999; Thomson and Delaney, 2001). In this model the blocks, buoyant remnants of a pre-existing icy crust, move about in a slushy matrix, both translating and tilting. Eventually the matrix freezes, ending the blocks' motions and preserving their final positions. Heights of the blocks (~200–300 m) above the lower-lying matrix material have been calculated through shadow measurements; these plus buoyancy physics then imply that the pre-existing icy crust was no more than several kilometers thick (Williams and

Greeley, 1998). To cause the melt-through, this model requires localized heating of the crust to be maintained for some period of time. Thomson and Delaney (2001) model Europa's ocean as weakly stratified[10] (compared with Earth's oceans), and argue that warm buoyant plumes can rise from volcanic regions on the ocean floor and reach the underside of the ice crust. Such plumes would be narrowly confined by the Coriolis force arising from Europa's rotation. Plumes with heat fluxes of $\sim 10^{11}$ W, perhaps $\sim$1% of Europa's global heat flux, could melt through the crust in $\sim 10^3$ yr.

An objection to localized melt-through events is Stevenson's (2000b) argument that a melt-through event would be impossible; the viscosity of warm ice is so low that adjacent ice would flow quickly enough to fill in any growing gap. This argument, while sometime stated categorically, does not apply to thin conducting shell models, for which only a very thin layer of ice at the base of the ice shell has a low enough viscosity to flow appreciably (O'Brien *et al*., 2002).

The solid-state formation model for chaos regions suggests that ice rises to the surface in a diapir, eventually disrupting the brittle surface, perhaps even causing surface melting (Head and Pappalardo, 1999). Partial melting might occur due to positive tidal heating feedback during the ascent (Sotin *et al*., 2002). Chaotic terrain may form over these areas of partial melting within a solid ice shell. The pits, spots, and domes on Europa, collectively sometimes called *lenticulae*, have been suggested as the surface expression of diapirs. Others have argued that these features are rather the early stages of chaotic terrain development (Greenberg *et al*., 1999). Convection models have focused on the size and spacing of these features as a way of determining the thickness of the (putatively) convecting layer (see Section 19.8). Such features could form either by the intrusion of liquid material near the surface (a laccolith) or by warm, solid-state material nearing the surface (a diapir). Pappalardo *et al*. (1998) suggest a diapir origin, based on their nearly uniform size ($\sim$10 km) and spacing distribution of the lenticulae. Greenberg *et al*. (1999), however, have suggested that the uniform size and spacing is an artifact of the classification process; they find no peak in sizes at $\sim$10 km but rather a continuous distribution. This topic remains a lively area of disagreement, hampered by the fact that Galileo imaged only $\sim$9% of Europa's surface at a resolution of 200 m or better. Since models for the formation of chaos regions have been proposed for both thin- and thick-ice regimes, and there is ongoing disagreement about the nature of the data for the lenticulae, these features do not resolve the thick ice/thin ice controversy.

[10] Weak stratification means that water density, which varies with temperature and salinity, changes only slightly with depth; the greater the density gradient, the more work is required to move a parcel up or down the water column.

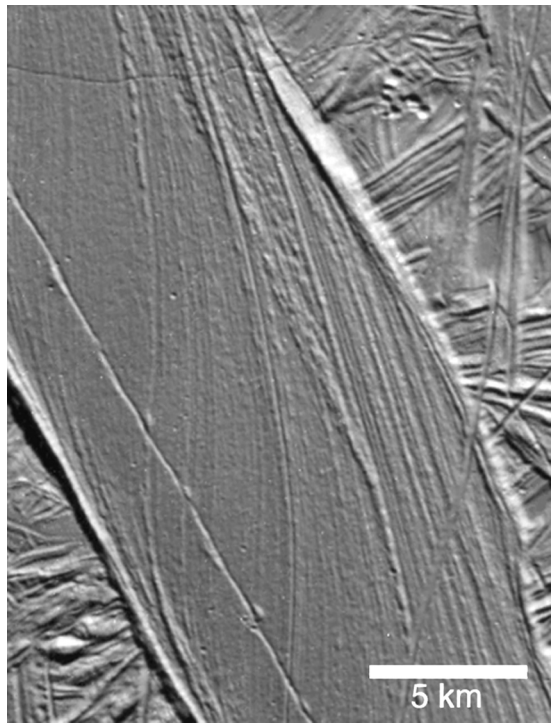

FIGURE 19.9 A band. Bands are similar to ridges, but appear to have been pulled apart laterally rather than built up vertically like double ridges. Bands can be up to 10 km wide, and hundreds of km long. This band shows small ridges inside of the main feature, perhaps formed as it spread apart.

19.7.4 Cryovolcanic flows and the "Puddle"

Cryovolcanic surface flows would be intriguing evidence for the presence of liquid water somewhere beneath Europa's surface, but there are few known candidate regions (Fagents *et al*., 2000; see Fig. 19.11 for one example). There is a buoyancy problem in their formation since it is difficult for liquid water, which is 10% denser than ice, to reach the surface. Diapirs have been suggested as formation mechanisms for various surface features on Europa, and one region, Murias Chaos (nicknamed the "Mitten"), could represent a location where warm, buoyant material was extruded onto the surface and flowed for a few kilometers (Figueredo *et al*., 2002).

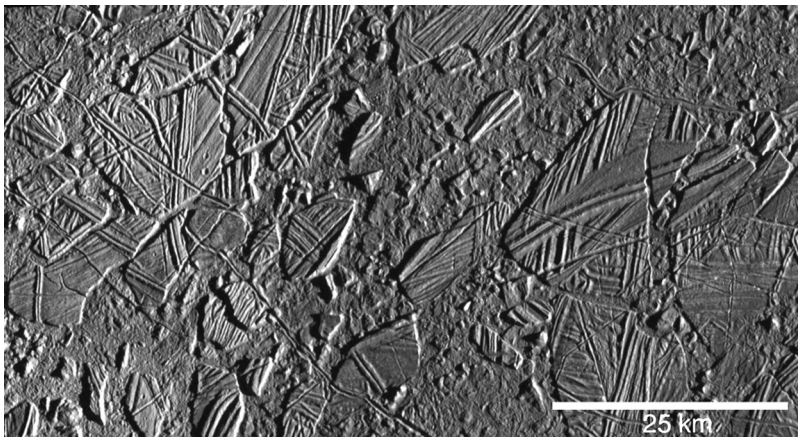

FIGURE 19.10 Conamara chaos. Disrupted, iceberg-like features are found in chaotic terrain. This image shows part of Conamara chaos, the defining feature of this type. Blocks of surface material seem to have broken apart, translated and rotated, and then refrozen in their new surface locations. The blocks can be reassembled like a jigsaw puzzle based on their shapes and features on their surfaces.

The "Puddle" is an intriguing, 3-km diameter feature (Fig. 19.11) where fluid-like material appears to have embayed (covered) pre-existing ridges and other terrain features. Underlying surface features are also visible inside the Puddle, suggesting that it consists of a thin surface veneer of fluid material that filled in low-lying regions, leaving ridges partially visible. The Puddle is one of only a few surface features exhibiting signs of cryovolcanism or other flow-like mechanisms. Small impact craters on the Puddle are secondary craters made by material thrown out by a large primary impact crater. No other geologic activity seems to postdate the formation of the Puddle.

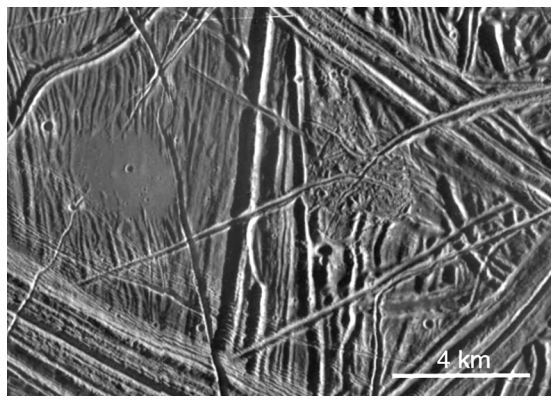

FIGURE 19.11 The "Puddle". The circular feature on the left side of this image, dubbed the "Puddle," is one of the few examples of a feature on Europa that could be the result of a cryovolcanic flow or eruption. The feature seems to embay (cover) the pre-existing terrain. Several small impact craters are visible on its smooth surface.

19.7.5 Craters

Europa's surface has very few large impact craters, as mentioned before, and those that are present are different from similarly sized craters elsewhere in the Solar System. The morphology of Europa's impact craters (see Fig. 19.8 for an example) suggests that they formed within a solid target, but their shallow depths imply that they have relaxed since their formation (Moore *et al.*, 1998). Such models suggest that most craters on Europa formed within a 5–15 km thick brittle surface layer, overlying a lower-viscosity subsurface layer. This subsurface material, however, could either be liquid water or warm, low-viscosity ice. More recent models attempt to use more subtle morphological details visible in Europa's craters to obtain better estimates of ice layer thickness. Turtle and Pierazzo (2001) modeled melt production and suggest that the ice crust must be at least 3–4 km thick to support the central peaks usually present. Schenk (2002) suggests that the ice shell could be 20 km or thicker, based on an interpretation of large, multi-ringed craters.

19.8 Heat transport and physics of the ice shell

Interpreting Europa's geology requires an understanding of the physics of Europa's ice shell. The deformation and flow of solids (*rheology*) is strongly dependent on temperature. Therefore, understanding Europa's surface features requires some knowledge of the ice shell's thermal structure, which in turn depends on how heat is applied to, generated within, and lost from the ice shell.

There are a variety of mechanisms for energy transport relevant to planetary bodies. *Conduction* is the transfer of energy by molecular collisions, and often dominates heat transfer in solids. It is a diffusive process in which molecules transfer their kinetic energy via collisions with other molecules. Heat will be conducted

wherever temperature gradients are present. *Convection*, by contrast, is transfer of energy via mass motion within the medium. Both conduction and convection seem plausible as means for heat transfer through Europa's ice shell. The temperature gradient within a shell whose surface temperature is ~100 K and whose base temperature must be that of Europa's ocean, ~270 K, will lead to heat conduction upwards from the warmer to colder ice. But it will also encourage convection, since the warm deeper ice will, because of thermal expansion, be more buoyant than the overlying colder ice. This creates a gravitationally unstable configuration that could lead, over geological timescales, to the rising of the warm ice and sinking of the cold in adjacent convection cells. Many geological materials are *viscoelastic*, meaning that they behave as an elastic solid on short timescales (e.g., Earth's mantle rock behaves elastically on timescales shorter than a few hours) but as a viscous fluid on long timescales (for Earth's mantle, timescales longer than 10^4 yr).

The physics of conduction and convection are discussed in Appendix 19.7. Proposed subsurface temperature profiles for Europa vary greatly depending on which meachanism dominates heat loss. Candidate profiles in Fig. 19.12 have implications for europan geology (since they affect the depth at which ice becomes sufficiently warm to be ductile) and for prospects for future remote subsurface probing within the ice shell (Section 19.9).

Other mechanisms for energy transfer are also important. *Radiation equilibrium* is the balance between energy absorption (from the Sun) and emission (roughly like a black body) that ultimately determines the temperature of Europa's surface. In addition, *tidal heating* acts to heat Europa's interior through energy transport from Jupiter's rotational kinetic energy and Europa's orbital energy (Appendix 19.3).

Models of the thermal state of Europa's icy crust show that solid-state convection will begin if there exists a thin, cold, brittle, stagnant lid over a sufficiently thick, warmer, ductile ice sublayer (McKinnon, 1999). The Rayleigh number *Ra* provides a criterion for the onset of convection – when conditions are such that *Ra* is greater than some value Ra_{crit}, convection occurs. The derivation of *Ra* and Ra_{crit}, and often overlooked assumptions in this derivation, are discussed in Appendix 19.7.

Early models suggested that if the ice layer were thick, solid-state convection would ensue, and the resulting heat transfer would rapidly freeze any ocean solid. Squyres *et al*. (1983) found the ice thickness needed for the onset of convection to be about 30 km. Their models combined three sources of heating to maintain Europa's liquid water ocean. Both tidal heating and radiogenic heating due to the decay of radioactive elements were taken to produce heat in Europa's core, combining to provide a heat flux at the base of the ocean of 16 erg cm^{-2} s^{-1} from the core. Tidal heating was taken to be uniform throughout the ice shell, and was the dominant heating term at 28 erg cm^{-2} s^{-1}. Thus the ice shell was heated from below by the tidal and radiogenic heating in the core (conveyed through the ocean) and from within by tidal heating. These effects combined to keep the ice layer thin, maintaining a liquid water ocean that lost its heat through conduction. Although available heating was insufficient to melt an ocean of water if ever it froze, if Europa started with liquid water, the ocean could be maintained as a liquid through geological time.

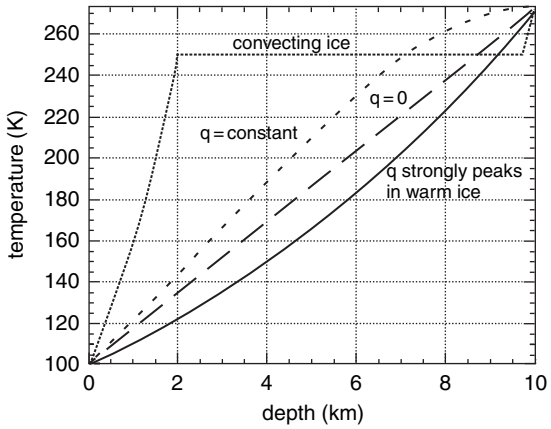

FIGURE 19.12 Theoretical temperature profiles in Europa's ice. The total ice layer thickness is assumed to be 10 km. The temperature profile labeled "convecting ice" is appropriate for an upwelling plume; descending plumes would be far colder. The volumetric heat dissipation rate *q* varies for different tidal heating models. (From Chyba *et al*., 1998).

Ojakangas and Stevenson (1989) extended this work to the case of more realistic ice rheologies in which tidal heating *q* within the ice shell depended on the product of the stress and strain rate; in this case *q* depended exponentially on temperature (see Appendix 19.7). More recent work has argued that convection is in fact the dominant mechanism for heat loss, and that conductive models alone cannot explain some of the surface features (Pappalardo *et al*., 1998). The thickness of an ice layer needed for the onset of convection has also been reconsidered. The viscosity of ice varies not only as a function of temperature, but also depends on strain rate, grain size, and other parameters.

Pappalardo *et al.* (1998) calculate that convection will occur if the subsurface layer is at least 2–8 km thick. They took the convecting layer to reside beneath a (geologically inferred) brittle *lithosphere*[11] less than 2 km thick. The observed 5–20 km spacing of supposed diapiric upwellings also supports a 2–8 km thick convection zone, since standard theory indicates that surface features should be about twice as far apart as the thickness of the convection zone.

It has been suggested that a change in ice thickness with time can be inferred from Europa's surface (Pappalardo *et al.*, 1998, McKinnon, 1999), since features such as the lenticulae, perhaps associated with a thicker crust, often crosscut (and are therefore younger than) ridges and tectonic features that are perhaps associated with a thinner crust. Changes in ice thickness through time are in fact predicted by coupled thermal–orbital evolution models of Europa (Hussmann and Spohn, 2004).

Virtually all geophysical models for Europa now include a subsurface liquid ocean. This is because (a) tidal heating theory and magnetometer data provide strong constraints, and (b) maintaining the warm ice needed for convection *without* ever creating a liquid water layer seems like a more extraordinary, fine-tuned set of conditions than the presence of a liquid ocean.

19.9 Future means for detecting an ocean

Future missions, especially with a Europa orbiter, could determine with certainty whether a europan ocean exists (Cooper *et al.*, 2002). An orbiting laser altimeter should be able to track details of Europa's deformation over each orbit. If a global subsurface ocean exists, the amplitude of Europa's time-varying tidal bulge as its distance from Jupiter slightly varies over an orbit will be as great as ~30 m, as opposed to only ~1 m if instead the water is all frozen down to the mantle (Moore and Schubert, 2000). Accurate spacecraft tracking would also allow measurement of higher-order terms of Europa's gravity field (Section 19.6.1; Appendix 19.1) by measuring the orbiter's response to the varying gravity field caused by the tidally deforming bulge. These measurements should also provide additional information about the satellite's internal structure.

[11] *Lithosphere* here refers not to rock, as its etymology would suggest, but to the brittle upper layer of the ice shell.

A more direct approach would be to orbit an ice penetrating radar. Detailed modeling indicates that a 20 W radar operating at 50 MHz could sound to depths of ~10 km in cold clean ice, but perhaps only to depths of several km if the ice is warm (~250 K) or if impurity concentrations are high (Chyba *et al.*, 1998; Moore, 2000). Fig. 19.12 shows that conductive ice temperature profiles are more favorable (because of colder temperatures to greater depths) than convective ice temperature profiles at the sites of upwelling plumes. However, very deep sounding might be possible at the locations of cold, descending plumes.

A Europa *lander* would present opportunities for different measurements. A single seismometer on the surface could passively monitor to determine the presence or absence of an ocean and estimate the thickness of the ice sheet (Kovach and Chyba, 2001). If two surface stations were available, coordinated seismic and magnetic measurements could not only detect the ocean, but also provide constraints on the ocean's thickness and on the deeper interior.

19.10 Habitability of Europa

Life as we know it on Earth depends on liquid water, a suite of "biogenic" elements (most famously C, but also H, N, O, P, S, Fe, and others) and a source of *free energy*, i.e., energy that is available and suitable to drive biological processes. As we have seen, it is likely, but not yet completely certain, that Europa harbors a subsurface ocean of liquid water whose volume is about twice that of Earth's oceans. Little is known about the inventory of carbon, nitrogen, and other biogenic elements, but lower bounds on their abundance can be placed by considering the role of cometary delivery over Europa's history (Pierazzo and Chyba, 2002). Sources of free energy may be limited for an ocean world covered with an ice layer kilometers thick (Reynolds *et al.*, 1983; Gaidos *et al.*, 1999), but it is possible that hydrothermal activity (McCollom, 1999) and/or organics and oxidants provided by the action of radiation chemistry at Europa's surface (Gaidos *et al.*, 1999; Chyba and Phillips, 2001; Cooper *et al.*, 2001; Chyba and Hand, 2001) and subsequent mixing into Europa's ocean could power a europan ecosystem. In this section, we assume the presence of liquid water in Europa's subsurface, and examine Europa's suitability for life from the perspective of biogenic elements and free energy. Figure 19.13 illustrates many of the processes discussed below.

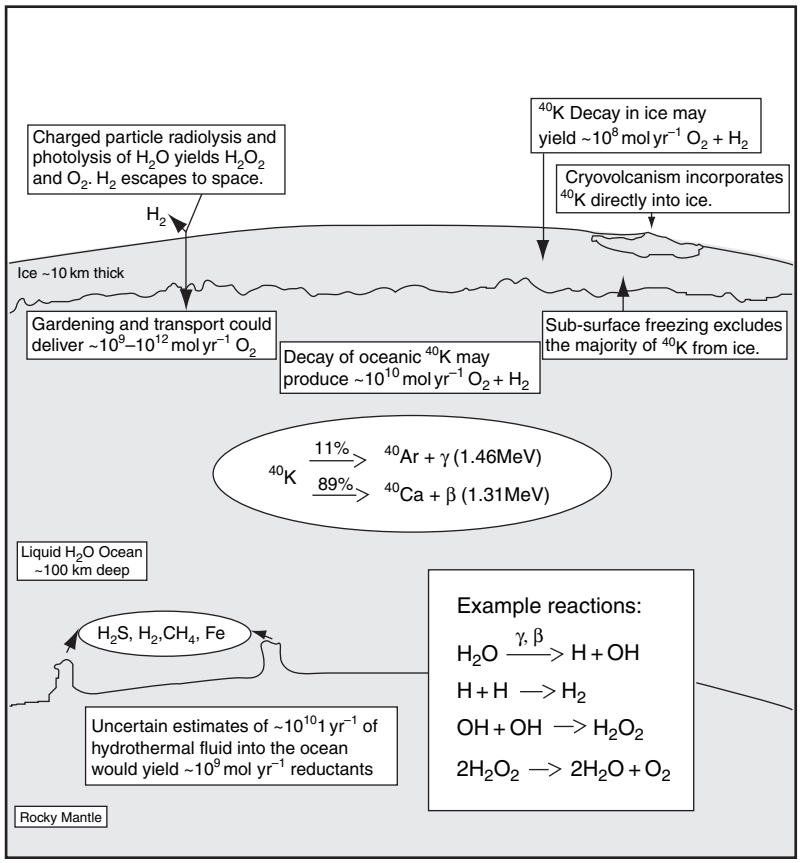

FIGURE 19.13 Free energy sources for life on Europa. Radiation effects on Europa's ice and liquid water could provide the chemical disequilibrium to fuel a biosphere. (After Chyba and Hand, 2001).

We will argue in this section that on the basis of what we currently know, Europa's putative subsurface ocean could be habitable by microorganisms with attributes similar to those known to exist on Earth. Habitability for extant life is not the same as suitability for the origin of life, as we have emphasized elsewhere (Chyba and Phillips, 2001), and will examine in the following section. However, Europa's apparent habitability presents an example of a world that is very different from one satisfying the traditional definition of habitability that relies on stable surface liquid water (Chapter 4). It appears likely that the biological arena may be much broader than that suggested by the traditional *habitable zone* definition, namely those circumstellar distances over which liquid water is possible on a planetary surface (Chapter 3; Sagan, 1996).

19.10.1 Biogenic compounds

In Section 19.5 we summarized the spectroscopic evidence for simple organic functional groups at Europa's surface, as well as the expectation that radiation acting on CO_2 in Europa's ice should produce simple organics such as H_2CO. A common default model for elemental composition of outer Solar System objects is that of a carbonaceous chondrite meteorite (perhaps with additional volatiles added); these meteorites are typically several percent organic by mass (Section 7.4.1). Such models for Europa's initial complement of organics (e.g., Kargel *et al*., 2000) must be viewed with caution, however, because the circum-jovian nebula in which Europa formed 4.6 Ga has a poorly known composition, and it may well have contained far less carbon, nitrogen, and other volatiles than carbonaceous chondrites.

Nevertheless, even if Europa was initially depleted in these biogenic elements, over Solar System history it would have acquired a considerable inventory of them via cometary impacts. While much material from such impacts would be lost due to Europa's low escape velocity, a significant fraction of lower velocity cometary material would be retained. Integrated over the history of the Solar System, Europa should have accumulated $\sim 10^{15}$ g of carbon in this way (Pierazzo and

Chyba, 2002) – ~0.1% of the carbon present in Earth's total mass of living organisms (*biomass*).

Because Europa lacks an atmosphere,[12] "soft landings" of interplanetary dust particles or small meteorites, sources that may have been important for the prebiotic organic inventory of early Earth (Section 3.8) or for the successful transfer of microorganisms between Earth and Mars (Section 18.4.4), will not occur on Europa. Delivery of intact organic molecules or viable microorganisms will therefore be far more difficult in the case of Europa. Moreover, the probability that material launched from Earth or Mars by impacts would reach Europa is far smaller than the probability of that material exchanging between Earth and Mars, though this is yet to be quantified. If life exists on Mars, it quite possibly shares a common ancestor with life on Earth, due to microbial transfer in meteorites; such common ancestry with terrestrial life is much less likely for life on Europa.

19.10.2 Photosynthesis

Photosynthesis on Europa is constrained by Europa's thick ice cover. It has been suggested that niches might exist within Europa's ice shell where transient near-surface liquid water environments could permit photosynthesis or other metabolic processes. Some models have as their context cracks or melt-throughs in a relatively thin, conducting ice shell (Reynolds *et al.*, 1983; Greenberg *et al.*, 2000), whereas another relies on dissipative heating in Europa's cracks (Gaidos and Nimmo, 2000) and works with either a conductive or convective model.

Were photosynthesis possible at Europa, for example if Europa's cracks permitted liquid water environments to reach sufficiently close to the surface, the energy available for biology from this source would likely swamp all others. Bacterial photosynthesis on Earth ranges over the wavelength range 360 nm to 1020 nm (Section 13.3); over this range nearly two orders of magnitude more energy is incident on Europa (globally averaged) in the form of photosynthetically useful photons than is incident in charged particles (Cooper *et al.*, 2001). This suggests that were life to exist on Europa, and were it to have access to near-surface liquid-water environments, there would be a strong selection pressure for the evolution of photosynthesis at any near-surface niches (such as cracks). The possibility that the reddish brown coloration of Europa's cracks or other disrupted terrain might be due to such microbial colonization has been a topic of speculation in the literature (Dalton *et al.*, 2003). However, without excluding this possibility, we caution that it is easy to attribute unexplained features to biology, since life's potential characteristics are poorly constrained.

This is not a new caution. Pollack and Sagan (1967) warned against the temptation to attribute enigmatic martian albedo features to biology: "The varieties of life on Earth and of possible organisms that we can imagine on Mars are so large that virtually any change in surface features can be 'explained' by a necessarily vague attribution to biological processes." In our view this does not mean that biological explanations are out of bounds, but rather that they require strong evidence before being accepted.

19.10.3 Hydrothermal vents and chemical disequilibria

Microbial life on Earth often does not directly harvest solar energy, but obtains its energy from other chemical disequilibria in the environment, bringing together an electron donor (a "fuel") with an electron acceptor (an "oxidant") to liberate energy (Chapters 6, 8, and 11). On Earth, photosynthesis, coupled with organic carbon burial, produces oxidizing surface conditions that provide chemical disequilibria for biology to exploit. Gaidos *et al.* (1999) emphasize the difficulty of identifying sources of chemical disequilibrium on an ice-covered world lacking photosynthesis, and the corresponding difficulty of sustaining a large biomass on Europa. Yet the Earth itself must have hosted a biosphere prior to the evolution of photosynthesis, so the absence of photosynthesis cannot be an insurmountable obstacle to maintaining chemical disequilibria that can provide the electron donors and acceptors to power life. Indeed, there may be elements of Earth's deep subsurface biosphere, for example hydrogen-consuming methanogens, that are entirely independent of surface photosynthesis (Chapelle *et al.*, 2002).

Early models for heating in Europa's interior suggested that the heat flow at the base of the ocean might be 24 mW m^{-2} (Squyres *et al.*, 1983). For comparison, the average heat flow at the surface of Earth's Moon is 29 mW m^{-2}, one-third of Earth's. Since the Moon is geologically dead, this simple comparison seems

[12] As discussed in Section 19.12.1, Europa may have had an atmosphere for its first 10^5 yr, but this would seem to be too short an interval for life to both originate somewhere else and undergo transport to Europa.

discouraging for hydrothermal activity at the base of Europa's ocean. However, more recent tidal models for Europa suggest the possibility of heat flows as high as $\sim$200–300 mW m^{-2}, in which case hydrothermal activity would be expected. In these models a liquid inner core for Europa allows more tidal flexing and so more heat production in the mantle, and the resulting large heat flows produce partial melting, resulting in volcanism at the interface between the ocean and mantle (McKinnon and Shock, 2001). If, however, the convective heat transfer in Europa's mantle is efficient enough to prevent partial melting of silicates, volcanic activity might be precluded.

If hydrothermal vent activity does exist on Europa, venting of CO_2 to the ocean seems plausible (McKinnon and Shock, 2001). This CO_2 could then serve as an electron acceptor, e.g., for molecular hydrogen produced by water acting on basalt. The methane-producing biomass that could be supported by such a system (Chapelle *et al.*, 2002) is difficult to calculate, but is likely small. McCollom (1999) estimates a potential annual biomass production of $\sim 10^8$–10^9 g yr^{-1} (using a dry biomass production energy efficiency $\varphi \sim 0.1$ g $kcal^{-1}$), vastly less than Earth's primary production based on photosynthesis of $\sim 10^{17}$ g yr^{-1}. The extent to which such an ecosystem, lying at the base of a 100-km deep ocean, would be detectable by measurements at Europa's surface would depend on the amount of vertical mixing in Europa's ocean. The model of Thomson and Delaney (2001) suggests that a great deal of mixing between ocean bottom and the ocean/ice interface might occur.

19.10.4 Chemical disequilibria from particle radiation and radioactive decay

A number of authors have discussed the production of oxidants (such as molecular oxygen and hydrogen peroxide) in Europa's uppermost ice layers due to charged-particle bombardment of water ice (Cooper *et al.*, 2001). Since CO_2 is also present in the ice (McCord *et al.*, 1998), there should be a simultaneous production of simple organics such as formaldehyde (Chyba and Phillips, 2001). The mixing of oxidants and organics into the europan ocean over the $\sim$50 Myr lifetime of Europa's ice shell would then make chemical disequilibrium energy available to the ocean.

The extent to which organics and oxidants produced at Europa's surface are available to power an oceanic ecosystem depends on the competition among charged particle and ultraviolet processing of the surface, sputtering and gardening (Section 19.3), and the communication of the surface layers with the oceans via geological processes. There are many uncertainties in such a calculation; estimating a biomass production rate further requires that the calculated energy available from fuel-oxidant reactions be combined with estimates of the efficiency φ of converting energy into microbial biomass (dry weight). Biomass production rates given below allow for an order of magnitude uncertainty in φ, ranging $\sim$0.1–1 g $kcal^{-1}$ (McCollom, 1999; Chyba and Phillips, 2001).

The more conservative estimates suggest that Europa's oceanic biomass could be limited to $\sim 10^{22}$–10^{24} prokaryote-like cells. In these conservative scenarios, it would be very difficult to supply the ocean with enough radiation-produced oxygen to reach levels capable of sustaining analogues to terrestrial macrofauna (Chyba and Phillips, 2001), which require O_2 concentrations above $\sim$20 μM. In this case, any europan ecosystem would be limited, assuming the validity of this analogy to terrestrial biology, to microscopic life. Estimates that assume that the available ice substrate somehow keeps pace with the intense radiation bombardment – so that the uppermost ice layers are constantly being replenished and substrate-limitation is never a factor – can increase the O_2 concentration by factors of 10^3 or more, comparable to that on Earth (Cooper *et al.*, 2001), and seemingly permit macrofauna.

Conductive models involving melt-through (Greenberg *et al.*, 2000) and convective models in which such nutrient-rich ice is circulated in the solid-state down to the ocean (Chyba and Phillips, 2001) may permit the upper meters of Europa's surface to mix with Europa's ocean. Barr and Pappalardo (2003) suggest that downward convective circulation in the ice could permit material from Europa's stagnant lid to be transported to the base of the ice shell in 10^4–10^7 yr, perhaps including the upper meter of ice. If Europa has hydrothermal vents that introduce reduced fluids into the ocean, then the production of organics or hydrogen in Europa's ice is not needed, and the oxidants would be provided by radiation chemistry at the surface. This difference in oxidation state could provide the chemical energy needed by chemolithoautotrophic microbes, as it does in vent systems on Earth (Chapters 8 and 14). The availability of O_2 could also allow a metabolism based on iron reduction and oxidation (Schulze-Makuch and Irwin, 2004).

Chyba and Hand (2001) have considered additional sources of oxidants and hydrogen on Europa. In

particular, they consider simultaneous production of oxygen and hydrogen in Europa's bulk ice and in the ocean itself due to the decay of radioactive ^{40}K, using the Kargel *et al*. (2000) model to estimate the concentration of potassium in Europa's ocean. This model assumes total extraction of salts from a carbonaceous chondrite precursor. Zolotov and Shock (2001) view this as unlikely, and present a range of other models; their favored model gives K concentrations ~30 times lower than that used by Chyba and Hand (2001). Taking this uncertainty into account, these processes could allow a biomass production of $\sim 10^8$–10^{12} g yr^{-1}. Sources of oxidants to Europa's ocean from the variety of radiation mechanisms considered here are summarized in Fig. 19.13.

Biomass production rates can be converted into estimates of steady-state biomass by using estimates of the biomass turnover time. For a turnover time of $\sim 10^3$ yr, perhaps appropriate for Earth's deep biosphere (Whitman *et al*., 1998), the above calculation permits a steady-state biomass of $\sim 10^{11}$–10^{15} g, compared with the terrestrial biomass of $\sim 10^{18}$ g.

19.10.5 Other sources of free energy

Other sources of free energy for life on Europa have been proposed in addition to photosynthesis and chemical disequilibrium. Scenarios for life based on electrical energy and thermal energy (Reynolds *et al*., 1983), as well as osmotic energy, kinetic energy, magnetic energy, gravitational energy, and piezoelectric energy have been considered (Schulze-Makuch and Irwin, 2004). Schulze-Makuch and Irwin conclude that osmotic and thermal gradients, as well as the kinetic energy of convection currents, represent plausible alternative sources of energy for life on Europa, although there are no known organisms on Earth that obtain their energy in these ways.

19.11 Europa as a possible analogue for early earth

Europa is of astrobiological interest primarily because of its potential as a habitat for extraterrestrial life. However, it may also provide a model for the early Earth at the time of the origin of terrestrial life. Stars like the Sun grow more luminous through time as the hydrogen in the star's core is converted to helium. Our Sun was ~25% less luminous 4 Gyr ago at the time of the origin of life, with the result that Earth's surface would likely have been frozen over unless there was a much stronger greenhouse effect at that time (Section 4.2).

One popular, but uncertain, solution to this "early faint Sun paradox" is to invoke much higher levels of the greenhouse gas CO_2 in early Earth's atmosphere. However, although this remains the favored resolution, there are reasons to remain skeptical about this solution (e.g. Sagan and Chyba (1997); Section 4.2 argues for CH_4 as the early greenhouse gas). A different possible resolution to the problem is to instead envision the early Earth as a world whose mean average temperature was only ~237 K. The resulting "Snowball Earth" may also have occasionally reappeared throughout terrestrial history (Section 4.2.4).

If this model of the early Earth is correct, somehow life must have originated and then flourished, even under these conditions (Bada *et al*., 1994). Europa provides a Solar System analogue for this model. Earth's early oceans, like those of Europa today, would not have frozen solid since the geothermal heat flux would have limited the thickness of the oceans' ice cover to an average 300 ± 100 m (via Eq. (19.25) in Appendix 19.7). Tidal heating of the ice itself would have been negligible since ice this thin is brittle, and only ductile ice can deform and be tidally heated. The challenge is to understand how the origin of life could have occurred either on such a Snowball Earth or perhaps on Europa.

19.12 An origin of life on Europa?

In Section 19.10 we argued that Europa's ocean appears habitable by microorganisms, but of course habitability by analogies to extant Earth organisms is not the same thing as life being present. Since it is unlikely that organisms have been successfully transferred between Earth and Europa (Section 19.10.1), life on Europa likely exists only if a separate origin of life took place there. The prospects for this are difficult to evaluate, especially given our limited understanding of the origin of life on Earth.

19.12.1 An early surface ocean?

One model for the formation of Ganymede, Callisto, and Titan suggests that these moons began with an atmosphere rich in water vapor and a correspondingly powerful greenhouse effect; however, in this model the resulting surface liquid water ocean rapidly cooled below the freezing point in $<10^5$ yr (Kuramoto and Matsui, 1994). Unless further modeling indicates that

the timescale for the existence of a surface ocean on Europa could be substantially longer, or that the origin of life on Europa could happen within this extremely short period, any life that originated on Europa must have done so beneath Europa's ice cover.

Conditions on Europa shortly after its accretion may have been different in other ways important for its habitability or for the origin of life, but these effects are difficult to evaluate. Radioactive heating in Europa's core should have been several times higher than today, which (everything else being equal) should have favored a thinner ice layer. Similarly, more left-over accretional heat should have been present, as well as heat from Europa's initial rapid despinning (Appendix 19.1). The cometary impact flux may also have been substantially higher, though models for the decay of the impact flux in the early outer Solar System are uncertain. Perhaps most important, the timing of the commencement of Europa's orbital resonances with Io and Ganymede, and the implications for tidal heating, is controversial (Appendix 19.4).

19.12.2 An origin of life in the subsurface?

If life in general cannot originate at depth, then only worlds that have clement surfaces sufficiently long for life to originate (Earth, perhaps Mars) can host endemic biologies, although interplanetary transfer of microorganisms remains possible. If life can originate at depth, however, then Europa might harbor its own endemic biology. Certain prebiotic processes under hydrothermal conditions may have been important in the origin of Earth's life (Chapters 8 and 14), but it remains unclear whether the entire origin of life could have proceeded in the absence of sunlight.

Just as Titan and Europa may provide partial analogues to early Earth environments of relevance to the origin of life, so carbonaceous chondrite meteorites may provide clues into the origin of life at depth. Most researchers conclude that these meteorites experienced liquid water, based on their mineralogy and the standard interpretation of their amino acid chemistry (Section 3.9.2). Asteroid thermal history models suggest that large asteroids ($\sim$100 km diameter) could maintain liquid water interiors for $\sim 10^8$ yr, but the best studied carbonaceous chondrite, the Murchison meteorite, probably experienced water for much less time than this, perhaps only $\sim 10^4$ yr (Chyba and McDonald, 1995). Such meteorites thus present actual examples of prebiotic organic synthesis in subsurface hydrothermal environments – they experienced liquid water, potentially catalytic mineral surfaces, and abundant organic molecules. Yet while over 75 types of amino acids are present in Murchison (Tables 7.1 and 7.2), only very low concentrations of even two-amino-acid chains have been found.

19.12.3 Advantages of ice

A number of authors have remarked that low temperatures (provided liquid water exists) may favor the origin of life. Bada *et al.* (1994) and Bada and Lazcano (2002) emphasize the enhanced stability of prebiotic organic molecules at low temperatures. For example, hydrogen cyanide (HCN) is often viewed as a critical precursor to the synthesis of both amino acids and nucleic acid bases, yet its half-life against hydrolysis is only a few years at 50 °C but 10^4–10^5 yr at -2 °C. Steady-state concentrations of key molecules would thus have been highest in a cold ocean or lake. Moreover, freeze–thaw cycles could have concentrated prebiotic reactants in spaces between ice crystals, offsetting the slower reaction rates at lower temperatures. There is now direct experimental evidence for this in the context of nucleic acid synthesis (Kanavarioti *et al.*, 2001). Similarly, Levy *et al.* (2000) find that some nucleic acid bases and amino acids are synthesized in substantial yields in dilute solutions of NH_4CN held at both -20°C and -78 °C for 25 years. These authors suggest that this demonstrates the potential for prebiotic chemistry on Europa or an ice-covered early Earth.

19.12.4 Effects of a salty ocean

Some models for Europa's ocean (Kargel *et al.*, 2000; Zolotov and Shock, 2001) imply that its salt concentration may be high enough to impede the origin of life (Hand and Chyba, 2007). Monnard *et al.* (2002) have shown that two processes relevant to the origin of life, membrane self-assembly and RNA polymerization, are both impeded by ionic solute concentrations much lower than even those of Earth's contemporary ocean (Section 19.6). They conclude that the origin of cellular life on Earth more likely occurred in a freshwater rather than a marine environment. For example, NaCl concentrations in the range of 80 mM (14% of present-day seawater) are sufficient to halve the longest RNA *oligomers*[13] formed in their experiments;

[13] An *oligomer* is a relatively short polymer, in this case containing a small number of nucleotides.

concentrations around 40 mM reduce the total yield of oligomers synthesized by a factor of two, and 25 mM NaCl substantially reduces RNA oligomerization. They point out that freezing mechanisms that act to concentrate organics may also concentrate salts due to the exclusion of salts from the freezing ice matrix (Chapter 15), suggesting that freezing in a salty ocean, as discussed above, may cause as many problems as it solves. However, melts that occurred within previously existing ice, perhaps due to tidal mechanisms (e.g., Gaidos and Nimmo, 2000; Sotin *et al*., 2002), may have low salinity because the ice already excluded most salts during its initial freezing.

Hand and Chyba (2007) derived empirical constraints on the salinity of Europa's ocean from the conductivities implied by the Galileo magnetometer measurements combined with geophysical models (Section 19.6). They find that these constraints are best met by a global layer of water with salt concentration in the range 1.3–115 g $MgSO_4$ or 0.8–39 g sea salt per kg H_2O, with the most likely values toward the low end of these ranges. For comparison, Earth's oceans have a salinity of $\sim$35 g kg^{-1} sea salt (mostly NaCl). That is, the magnetometric and gravity measurements at Europa are most likely satisfied by an ocean that is not strongly saline, and that could even satisfy the terrestrial definition of freshwater. We conclude that the salinity of Europa's present ocean appears could well be small enough that it would not impede prebiotic reactions needed for the origin of life.

19.13 Searching for life

Any search for life on a distant world must establish criteria for what would qualify as evidence of success. But no general definition of life has been accepted by the scientific community (Chyba and McDonald, 1995). There appear to be fundamental philosophical reasons having to do with the nature of definition and our current understanding of life for why no compelling definition is currently possible (Chapter 5). This has implications for how we should search for life at present, as does the one historical example we have of the search for extraterrestrial life from a spacecraft, that conducted by the Viking project in 1976 (Sections 18.5.2 and 23.2).

19.13.1 Possible missions

We regard europan exploration as comparable in importance to that of Mars, demanding a systematic program of exploration. Mars is a target of such importance that its exploration requires multiple missions over many decades; these missions are interwoven in a way that incorporates new knowledge into an existing program. Missions to Europa are necessarily more challenging and expensive than missions to Mars, but a program of europan exploration need not launch to Europa every two years, which is the current pace of Mars exploration. A wide variety of missions to Europa has been envisioned.

The first lander on Europa – which may well be preceded by an orbiter or flyby mission (Cooper *et al*., 2002) – should touch down at a site where liquid water from Europa's subsurface may have recently reached the surface. The locations, or even existence, of such sites are difficult to determine with confidence on the basis of current knowledge, but if we had to choose a landing site now, we might well choose a feature like the Puddle described in Section 19.7.5 (Fig. 19.11). Information from an orbiter mission would obviously be of great help in answering these questions.

A search for subsurface europan life via measurements performed on Europa's surface should examine ice from the youngest possible surface. Prior to or simultaneous with any experiments to search for life, chemical context should be established. This is a clear lesson from the Viking missions to Mars (Section 18.5.2; Chyba and Phillips, 2002). Measurements would include determining the abundance of cations and anions, salinity, pH, volatiles (O_2, CO_2, CH_4, etc.), and organic molecules. The last is probably the highest priority "life-detection" experiment to be performed. Additional experiments could include high-sensitivity searches for specific indicative organic molecules (such as amino acid enantiomers), determination of key stable isotope ratios (e.g., $^{12}C/^{13}C$), or fluorescent microscopy. Searches for organic molecules should be made at the greatest depth into the ice as possible, because laboratory experiments suggest that radiation near the surface will destroy the less stable biomolecules on short timescales (Bada and Lazcano, 2002).

The biological models described in Section 19.10 suggest that europan biomass may be limited. This suggests that any search for life on Europa from a lander should either survey a large amount of material so as to choose particular locations for subsequent high-sensitivity investigations, and/or take advantage of the opportunity to concentrate samples by melting and filtering ice. Chyba and Phillips (2002) have

discussed the energy requirements for the latter strategy on Europa, and consequent limits on how much material might be processed.

Finally, even without landing it would be possible to sample the surface with a mass spectrometer to analyze either material sputtered off the surface (Johnson, 1998) – though this material will be the most heavily radiation processed – or blown off the surface by an artificial impact (Cooper *et al*., 2002). Such a flyby mission would have the advantage of being less technically demanding and much less costly than an orbiter or lander.

19.13.2 Preventing contamination of Europa

There is both a legal requirement and a practical scientific objective that any environment to be searched for life not be contaminated with "false positives" inadvertently brought along from Earth. We also believe that "planetary protection" requirements flow from an ethical obligation to avoid significantly contaminating possible alien biospheres (see Chapter 25 for a full discussion).

It is credible that microbes within a terrestrial spacecraft could reach Europa and remain viable. Experiments conducted aboard a number of Earth-orbiting spacecraft indicate that a variety of common terrestrial bacteria can withstand the space environment for as long as six years provided they are shielded from ultraviolet light (Horneck, 1993). After travel through interplanetary space, the microbes would then have to (1) survive the jovian radiation environment (Section 19.4.1) during flyby or while in orbit around Europa, (2) be delivered to Europa's surface, (3) be buried in Europa's ice quickly enough so that at least some would survive the surface radiation environment, and (4) be transported into Europa's ocean (either by cracking, melting, descending plumes, or some other mechanism; see Section 19.7). Finally, and perhaps most challenging of all, (5) at least one of these organisms would then have to be able to survive and reproduce in the ocean.

In the 1970s values for such probabilities were adopted for Mars, but then later criticized as subjective and uncertain by the US National Research Council's Task Group on Planetary Protection (Space Studies Board, 1992). For Mars missions the 1992 study adopted mission categories that in general required Viking lander presterilization (clean room) requirements and, for missions that would search for life, Viking lander sterilization requirements (which added day-long baking at 110 °C) (Section 25.6). A later Task Group on the Forward Contamination of Europa attempted to quantify the probabilities for four classes of microorganisms. Majority opinion was that a more quantitative and potentially more stringent requirement was needed: that the probability be 1 in 10,000 for any mission to contaminate a europan ocean with a viable terrestrial microbe (Space Studies Board, 2000). They argued that this criterion can be met even with minimal ground-based sterilization of the spacecraft, largely because of the post-launch sterilization effects of Europa's radiation environment.

Critics of this report suggested that the requirement should be based on a more transparent criterion, such as requiring the probability of contamination to be "substantially smaller than the probability that such contamination happens naturally." This could prove an extremely stringent requirement in the case of Europa, a world to which viable microbial transfer in terrestrial meteorites is likely extremely difficult (Section 19.10.1). However, the probability of natural contamination still needs to be carefully modeled. We are unlikely to launch more than ten missions (and probably fewer) to Europa before we either determine that a biosphere exists or lose enthusiasm for further europan exploration, so that the 10^{-4} contamination probability requirement (per mission) would mean that the chances of contaminating Europa for all missions would be $\sim$0.1%.

19.14 Europa and astrobiology

In this chapter, we have tried to distinguish between what is known with confidence, what is likely to be true, and what is speculative. It seems virtually certain that Europa has a $\sim$100-km thick layer of H_2O on its outer surface. It is likely that most of this water is liquid, comprising an ocean whose volume is roughly twice that of Earth's oceans. The evidence for this picture is strong but still indirect. Europa seems likely to be habitable in the sense that it probably has liquid water, biogenic elements, and sources of free energy capable of sustaining life. Europa also provides an analogue to at least one class of models for the Earth at the time of the origin of life. Europa thus joins Mars as the two most likely environments for extraterrestrial life in our Solar System. In one sense, the possibility of life on Europa seems the more intriguing, since were it present it would likely represent an origin separate from life on Earth.

None of this means, of course, that there is in fact a europan biosphere. It is extremely difficult, given

our poor understanding of the origin of life, or the prospects for the origin of life in subsurface environments, to estimate the likelihood of the origin of life on Europa. The only way we will discover whether there is life on Europa is to go there and find out.

Appendix 19.1 Satellite tides and synchronous rotation

This appendix explains the physics of Europa's tidal torques and how they lead to synchronous rotation.

A point P on Europa experiences a force $\mathbf{F}_J$ due to Jupiter's gravity corresponding to an acceleration $\mathbf{a}_J = GM_J d^{-3}\mathbf{d}$, where G is the gravitational constant, M_J is Jupiter's mass, and $\mathbf{d}$ is the vector distance from the point P to the center of Jupiter. (Boldface type denotes vector quantities.) P also experiences a centripetal acceleration $\mathbf{a}_c$ as it, along with Europa, orbits the system's center of mass. The difference between the two accelerations, $\mathbf{a}_T \equiv \mathbf{a}_c - \mathbf{a}_J$, is called the *tidal acceleration*, and it is not difficult, though trigonometrically tedious, to calculate $\mathbf{a}_T$ explicitly (e.g., Murray and Dermott, 2001, Section 4.2). Because $\mathbf{F}_J$ falls off with the square of the distance, the side of Europa nearer Jupiter experiences $|\mathbf{a}_J| > |\mathbf{a}_c|$, with the situation symmetrically reversed on the far side where $|\mathbf{a}_J| < |\mathbf{a}_c|$. The magnitude of the difference is greatest at the points nearest and farthest from Jupiter. The result is that Europa's figure experiences a position-dependent tidal force that distorts it into a prolate spheroid with its major axis oriented toward Jupiter. (Put another way, Europa is stretched along the radial line to Jupiter because the *difference* in $\mathbf{F}_J$ experienced by one point at a distance x from Jupiter's center and another at a distance $x+\delta x$ is proportional to $x^{-2} - (x+\delta x)^{-2} \approx 2(\delta x)x^{-3}$). That is, the tidal bulge is symmetric on both the subjovian and antijovian sides of Europa, and is proportional to the inverse cube of the distance to Jupiter. The magnitude of the distortion depends not only upon $\mathbf{F}_J$, but also on Europa's gravity and rigidity, which resist the distortion.

Gravity is a conservative force, so the vector $\mathbf{a}_J$ can be written as the gradient of a scalar potential, as can the centripetal acceleration. Tidal calculations are usually framed in terms of gravitational potential functions; forces and accelerations can be determined by taking the gradient of their potential. Ignoring a constant, we can then express the tidal acceleration $\mathbf{a}_T$ as $\mathbf{a}_T = \nabla V_T$, where V_T is Jupiter's tide-raising potential. For spherical coordinates r_e and θ with respect to the center of Europa, and to second order,

$$V_T(r_e, \theta) = -(GM_J r_e^2 / r_{eJ}^3) P_2(\cos\theta), \qquad (19.1)$$

where $P_2(\cos\theta) = (1/2)(3\cos^2\theta - 1)$ is the second degree Legendre polynomial and r_{eJ} is the distance between the centers of Europa and Jupiter (Stacey, 1977).

The distortion of Europa's surface caused by the potential V_T is $\delta(\theta) = h_2 V_T(\theta/g)$ (giving a prolate spheroid), where g is Europa's gravitational surface acceleration and h_2 is the tidal Love number, which corrects for the rigidity of Europa and a second degree disturbance of the tidal potential due to the deformation itself. For a homogeneous sphere of radius r_e, density ρ, and rigidity μ, a measure of the force needed to deform an elastic body is:

$$h_2 = (5/2)[1 + 19\mu/2\rho g r_e]^{-1}.$$

Now consider Europa early in its history, when its rotational period was likely shorter than its orbital period about Jupiter. (If its rotational period were in fact longer, an analogous argument to the one given below would apply and give the same conclusion.) As each longitudinal section of Europa rotates past the Europa–Jupiter radial line, the tidal bulge of this section rises to maximum height and then falls. If Europa could deform instantaneously in response to the tidal potential, the tidal bulge would always be perfectly aligned with the radial line to Jupiter, and there would be no net torque acting on Europa's tidal bulge. Since no real material can deform instantaneously, however, Europa's elastic response lags behind the periodic tidal potential, resulting in an angular offset of the maximum bulge a bit past the subjovian point (Fig. 19.2). This offset tidal bulge produces a torque. Since gravity falls off with distance, the torque is slightly greater on the bulge nearer Jupiter (tending to slow down the rotation) than on the symmetric bulge on Europa's far side (tending to speed up the rotation). The sum of the torques therefore does not quite cancel, and acts to "despin" the satellite, i.e., slow down its rotation.

The distorted shape of Europa leads in turn to a distortion in its own gravitational potential field, introducing a quadrupole term

$$V_D(r_e, \theta) = k_2 V_T(\theta)(r_e/a)^3, \qquad (19.2)$$

where k_2 is called the second-order gravitational Love number; for a homogeneous sphere, $k_2 = (3/5)h_2$. Europa's total potential at point (r,θ) then becomes $V_e = Gm_e/r + V_D(r,\theta)$. The magnitude of the torque Γ acting to despin Europa is becomes

$$\Gamma = |\mathbf{r}\ \mathbf{F}_J| = rM_J(1/r)(\partial V_D/\partial\theta), \qquad (19.3)$$

evaluated at $r = r_{eJ}$ and $\theta = \varepsilon$, where ε is the tidal lag angle (Fig. 19.2). One finds from Eqs. (19.1) to (19.3),

$$\Gamma = 3/2\ k_2 G M_J^2 r_e^5 r_{eJ}^{-6} \sin\ 2\varepsilon. \qquad (19.4)$$

This torque acts to despin the satellite until its rotation period becomes identical to its orbital period ($\omega = n$), after which $\varepsilon = 0$ and the system is in equilibrium. The satellite is then in synchronous rotation with its primary (as is the Moon with the Earth). The despinning timescale τ for Europa to become spin-locked with Jupiter is given by dividing its primordial spin angular momentum $C\omega_0$ by the despinning torque: $\tau = C\omega_0/\Gamma \propto r_{eJ}{}^{-6}(\sin\ 2\varepsilon)^{-1}$, where $C = \alpha m_e r_e{}^2$ is the moment of inertia, ω_0 is the intial spin angular velocity, and $\alpha \approx 0.35$ for Europa (see Appendix 19.5).

The energy dissipation rate in Europa from its periodic tidal forcing is related to the lag angle ε. The effective tidal dissipation function Q^{-1} is defined as

$$Q^{-1} = \frac{1}{2\pi E_0} \oint (-\dot{E}\ )\mathrm{d}t \equiv \frac{\Delta E}{E_0}, \qquad (19.5)$$

where $\dot{E}$ is the rate of energy dissipation, E_0 is the peak potential energy stored in the tidal bulge, and the integral extends over one tidal period (Goldreich and Soter, 1966). Q^{-1} is the part, ΔE, of the total energy stored, E_0, dissipated in a complete tidal period.[14] Integrating $\dot{E}$ for a sinusoidally varying external potential with a phase lag 2ε in the amplitude of the tidal motion, one finds $Q^{-1} = \tan(2\varepsilon)$ (MacDonald, 1964, Section 6). Since Q is generally large, $Q^{-1} \approx \sin(2\varepsilon) \approx 2\varepsilon$. As we will see below, Q for Europa is a matter of some controversy, but $Q \approx 100$ may be a reasonable guess for icy satellites in general (Squyres *et al.*, 1985). Europa's despinning must then have been extremely rapid, causing substantial but short-lived early tidal heating due to dissipation, perhaps as short as $\tau \sim 10^3\ (Q/100)$ yr.[15]

[14] Some authors define Q to be one-half the value used here.

[15] There are two different, and not entirely mutually consistent, formulations for Q in the literature. The approach used here dates to MacDonald (1964), and assumes that the satellite's tidal bulge is always offset from the line to the primary by a constant angle of magnitude ε whose sign depends only on the sign of the difference between ω and n. In a different formalism, called Kaula perturbation theory and dating back to George Darwin (son of Charles), coordinates of the perturbing potential are complicatedly but spectacularly transformed from spherical polar coordinates into polynomial functions of the orbital elements (Kaula, 1966).

Appendix 19.2 Tidal circularization of orbits and nonsynchronous rotation

Consider the effects of tidal heating (dissipation of energy) in a satellite that is spin-locked but in an eccentric orbit (Burns, 1976). The *specific* (per unit mass) *angular momentum* H for an orbit of semimajor axis a and eccentricity e is

$$H = [GM_J a(1 - e^2)]^{1/2}, \qquad (19.6)$$

and the *specific energy* of the orbit is

$$E = -GM_J/2a. \qquad (19.7)$$

The radial component of the tide (along the line connecting the centers of Europa and Jupiter) causes energy loss without causing a torque, that is, while conserving H. As E decreases due to energy dissipation, a must also decrease (the energy of the bound orbit becomes more negative), so that for H to remain constant, e must decrease as well, (by Eq. 19.6), leading to orbit circularization. For a given H, a circular orbit ($e = 0$) has the smallest a, so the minimum (largest negative) energy. Orbit circularization is opposed by the effect of torques due to tides raised by the satellite on the planet (called "planet tides"), but in most cases dissipation due to satellite tides dominates planet tides, and drives the eccentricity to zero (Goldreich and Soter, 1966).

For Europa, however, its eccentricity (and therefore tidal heating) is nonetheless kept from reaching zero by its orbital resonance with Io and Ganymede (Appendix 19.4). This may have important implications for Europa's spin rate. In Appendix 19.1 we showed that tidal evolution should lead to despinning of Europa on extremely short timescales. However, synchronous rotation is not necessarily the final rotation state for satellites whose orbits have nonzero eccentricity. The orbital distance from its primary of a moon in an eccentric orbit varies from $a(1 - e)$ to $a(1 + e)$. Because tidal torques (Eq. 19.4)) vary so strongly with the Europa–Jupiter distance, the torque Γ around Europa's orbit does not average to zero. In fact, $\langle \Gamma \rangle = (171/8\pi)\ k_2 G M_J{}^2 r_e{}^5 r_{eJ}{}^{-6} Q^{-1} e$ (Goldreich, 1966; Greenberg and Weidenschilling, 1984). The average torque is positive, since the torque is positive at perijove (point closest to Jupiter) where the tidal bulge is largest. This net nonzero torque may result in nonsynchronous rotation.

Were Europa's orbit circular, $\langle \Gamma \rangle$ would average to zero. Even for $e \neq 0$, however, synchronous rotation often occurs, due to counter-torques from permanent asymmetries in the satellite. In such a case a mean

deviation from spherical symmetry (e.g., due to an internal mass distribution asymmetry or a surface bulge) gives rise to a torque that balances the net nonzero tidal torque when the axis of minimum moment of inertia (e.g., the long axis of an ellipsoid) is oriented slightly off the direction to the planet. This orientation is stable and depends on the magnitude of the internal mass asymmetry and $\langle\Gamma\rangle$ (Greenberg and Weidenschilling, 1984). Most rocky bodies easily support such local mass asymmetries and so may be despun to synchronous rotation even for orbits with $e \neq 0$. Consider Earth's Moon, which maintains its synchronous rotation despite its eccentric orbit ($e = 0.055$) because substantial mass asymmetries are present. On the other hand, Europa has a thin ice shell incapable of supporting topography of much relief, and the ice shell is decoupled from its rocky interior by a liquid ocean. One could have mass asymmetries in the rocky interior that spin-lock the interior to Jupiter even while the ice shell responds to $\langle\Gamma\rangle \neq 0$ and rotates non-synchronously.

Such non-synchronous rotation has been invoked to explain the orientation of tectonic features on Europa's surface that are thought to have formed due to tidal fracturing of the surface, but which are not in locations or orientations currently coinciding with the greatest stresses predicted by tidal modeling. Geissler *et al*. (1998) unravel the ages and orientations of linear features in a northern high-latitude region of Europa, and find evidence for a systematic clockwise rotation of feature orientation with time that is consistent with Europa's surface spinning faster than synchronous and being decoupled from the interior.

A search for evidence of this non-synchronous rotation by comparing feature locations from Voyager to Galileo images provides a lower limit of $\sim 10^4$ yr for this rotation period (Hoppa *et al*., 1999c). Greenberg *et al*. (1998) found that the lineament orientations examined by Geissler *et al*. (1998) suggested that Europa had rotated about 60° during the time that these tectonic cracks formed. For an estimated surface age for Europa of ~50 Myr from cratering studies (Section 19.3.3), this suggests that Europa's non-synchronous rotation period may be some tens of millions of years, although a later study (Kattenhorn, 2002) suggests a much longer period.

If cracks form only under favorable tidal flexing conditions, then at any given time there is a limited set of locations and orientations where such features will be active. In the Greenberg *et al*. (1998) model in which cracks provide conduits of liquid water to Europa's surface, non-synchronous rotation has implications for possible biological niches in the cracks (Section 19.10). At most, organisms living in cracks would have millions of years before their habitat became inactive (and frozen) and they were forced to hibernate or migrate to a more favorable location (Greenberg *et al*., 2000).

The positions and orientations of various features have also been argued as evidence for *polar wander*, in which a decoupled ice shell slowly reorients itself in a north–south direction, producing an apparent change in position of the poles with respect to surface features (Sarid *et al*., 2002).

Appendix 19.3 Tidal heating

A satellite orbiting its primary will have a fixed tidal bulge with its axis of symmetry pointing towards the primary. If the satellite is in an eccentric orbit, there will also be *radial tides* (due to the tidal bulge rising and falling with respect to the fixed bulge as the satellite's distance from the primary varies around the orbit) and *librational tides* (due to the oscillation of the tidal bulge across the surface of the satellite as its velocity varies about the eccentric orbit). There may also be *obliquity tides* if the satellite has an obliquity, that is, if the obliquity angle θ between its axis of rotation and the orbit normal is nonzero. In this case the tidal bulge will also oscillate above and below the satellite's equator throughout an orbit.

All of these tides cause dissipation of energy within the satellite, i.e., tidal heating $\dot{E}$. If ΔE is the energy dissipated in the satellite over one tidal cycle (one rotational period T of the satellite), for a synchronously rotating satellite we may write $\dot{E} = E/T = nE/2\pi$ or, by Eq. (19.5), $\dot{E} = E_0(n/Q)$, where E_0 is the peak energy stored in the tidal bulge. For a Keplerian orbit, $n^2 = (GM_J + m_e)a^{-3}$. Calculating $\dot{E}$ exactly is complicated; it was first done for Earth's Moon in a model of a homogeneous, incompressible sphere, and extended to a two-layer lunar model in which a rigid mantle overlies a soft core (Peale and Cassen, 1978). This model turned out to be readily adaptable to a subsurface ocean model for Europa.

For an incompressible homogeneous satellite of radius r_e, tidal dissipation is given by (Murray and Dermott, 2001):

$$\dot{E} = 3/2(n/Q)k_2 GM_J^2 r_e^5 a^{-6}(7e^2 + \sin^2\theta), \qquad (19.8)$$

where the various quantities were defined in Appendix 19.1. This model was used by Peale,

Cassen, and Reynolds (1979) to predict volcanism on Io, then applied to the case of Europa (Cassen *et al.*, 1982), in which a function ($f\, r_c/r_e$) was introduced as a factor on the right-hand side of Eq. (19.8). This function determines the ratio of total dissipation in a mechanically decoupled shell (such as an ice layer floating on a liquid water core of radius r_c) to dissipation in a homogeneous world (Peale and Cassen, 1978). As r_c/r_e increases from 0 to 1, for realistic parameter values ($f\, r_c/r_e$) increases nonlinearly by over an order of magnitude (Cassen *et al.*, 1982). Physically, dissipation increases because, in the case of Europa, the distortion of the ice shell is much greater when it rides over a liquid ocean than it would be over ice. Indeed, estimates of the time-varying tidal bulge amplitude for Europa range from about 1 m for a solid ice shell with no liquid water layer to about 30 m for tens of km of ice over a liquid water layer (Moore and Schubert, 2000).

More recent theoretical work specific to tidal heating on Europa has focused first on modeling the tidal heating of the ice shell in a more realistic fashion, then on reconsidering the heating of Europa's core. Ojakangas and Stevenson (1989) calculated the energy dissipation in Europa's ice shell for two different candidate ice rheologies, assuming that heat loss through the ice occurs via conduction. The dissipation depends on ice viscosity, which in turn depends exponentially on temperature; the result is that tidal heating is strongly concentrated in the lowest, warmest layer of the ice shell. Indeed, the resulting temperature distribution in the ice shell is exponential with depth (Chyba *et al.*, 1998), rather than the linear temperature gradient familiar for a conductor heated simply from below. Heating of the ice varies as a function of latitude and longitude by a factor of five or so. Uncertainties in these models (Ojakangas and Stevenson, 1989; McKinnon, 1999) arise because the rheology of ice is poorly known at very low temperatures and at the low frequencies (corresponding to Europa's 3.6 day orbital period) associated with tidal flexing. Also unknown are the physical state of Europa's ice, especially its grain size and degree of fracturing, as well as its composition: the addition of small quantities of volatiles such as ammonia or salts to the ice could dramatically alter its viscosity.

As discussed in Section 19.10.3, models indicate that europan heat fluxes could be as high as $\sim$300 mW m^{-2} (McKinnon and Shock, 2001). Or, if one simply uses Eq. (19.8) to scale from the net tidal heating rate measured for Io (10^{14} W) to Europa's silicate/metal interior, one finds a value of 190 mW m^{-2} (O'Brien *et al.*, 2002).[16] Tidal heating may also vary substantially through time (Hussmann and Spohn, 2004).

Appendix 19.4 Orbital resonance and the Laplace resonance

The orbital periods of Io, Europa, and Ganymede are in a ratio of 1:2.007:4.045, very close to the integer ratios 1:2:4 (Fig. 19.4; Table 19.1). There are many examples in the Solar System where just two satellites have orbits near an analogous 1:2 commensurability.

Any small-integer commensurability leads to periodic mutual perturbations, whose effects are reinforced through repetition. In such a case, the perturbed satellite's natural frequency (given by its orbital mean motion $n = 2\pi/T$, where T is the orbital period) is nearly proportional to the forcing frequency (the frequency of strongest mutual gravitational interaction) of the system. As with many physical systems, when the forcing frequency and the natural frequency are nearly equal, a resonance results, referred to in this case as an "orbit–orbit" resonance. If the resulting enhanced mutual perturbations maintain the commensurability against other disruptive influences, the resonance is *stable*, or *locked*.

Here we examine the basic physics of orbit–orbit resonances. We restrict ourselves to a simplified description of a resonance involving only two satellites, since most of the important physics can be illustrated in this simpler system. At the end of the discussion, we will return to the three-satellite Laplace resonance of the jovian system.

Consider two satellites orbiting a primary. Subscript 1 labels variables pertaining to the inner satellite s_1, and 2 is for the outer satellite s_2. The natural frequency of s_1's orbit is just its mean motion n_1. The forcing frequency of the gravitational perturbation s_1 experiences because of the close approaches of s_2 is given by the difference $n_1 - n_2$, which measures the mean motion of s_1 as seen by an observer orbiting with s_2. Resonance will occur if the period of the natural frequency is an integer multiple of the forcing

[16] This scaling's validity depends, *inter alia*, upon whether heat flows resulting from Io's partially melted interior are reliably extrapolated to Europa. Since partially melted interiors result in greater tidal heating, which in turn makes a partially melted interior more credible, the extrapolation in some sense assumes its conclusion. These very different tidal heating estimates have important implications for both the thickness of Europa's ice layer (predicted to be as thin as 2 km for the most extreme value of heat flow cited here) and prospects for hydrothermal activity at the floor of its ocean.

frequency, or when $n_1 = j(n_1 - n_2)$, where j is an integer. This gives the resonance condition $(n_1/n_2) = (T_2/T_1) = j/(j-1)$ – resonance will occur if the mean motions (or equivalently, periods) of the satellites are in the whole number ratios $j/(j-1)$. In the case where $j = 2$, for example, s_1 orbits twice for every single circuit of s_2, so that a conjunction between the two satellites at a particular position (called the longitude of conjunction) in their orbits will be followed by a conjunction at the same orbital longitude a time t later, given by $n_1 t - n_2 t = 2\pi$, or $t = 2\pi/(n_1 - n_2) = 2\pi j/n_1 = jT_1$. Such an orbital commensurability exactly satisfies the condition of resonant forcing.

Now consider the net effect of this resonance (Murray and Dermott, 2001). We first try to explain the effects physically, then proceed to a more formal account. For illustration, consider the special case where s_1 has negligible mass and is moving in an eccentric orbit whose pericenter (the point in its orbit closest to the primary) has longitude (ϖ_1, and s_2 is moving on a circular orbit in the same plane (Fig. 19.14). Consider a conjunction of s_1 and s_2 that occurs shortly after s_1 has passed pericenter. (Refer to Fig. 19.3 to review the definitions of orbital elements used in this example.) The orbital elements of s_1, including its semimajor axis a_1, eccentricity e_1, and longitude of pericenter ϖ_1, will change as a result of this encounter. Because a and n are related by Kepler's third law according to $n^2 = G(M_J + m_e)a^{-3}$, n_1 and T_1 must change as well.

It is not hard to see why a_1 and e_1 must change. Consider the case of a conjunction that occurs when the objects are moving away from pericenter (Fig. 19.14). They are converging in their orbits because s_1 is moving outward from the primary. s_1 experiences a force $\mathbf{F}$ due to s_2; this force has both radial component $\mathbf{F}_r$ and tangential component $\mathbf{F}_t$. Exactly at conjunction $\mathbf{F}$ is purely radial and in an outward direction. This acts to increase the energy of s_1's orbit, therefore increasing a_1 and decreasing n_1. Since n_1 has decreased with negligible impact on n_2, the subsequent conjunction of s_1 and s_2 must occur sooner in s_2's orbit: conjunction after conjunction, the longitude of conjunction is pulled slowly back toward pericenter.

A similar analysis for a conjunction that occurs immediately *prior* to pericenter shows that in this case the longitude of conjunction is pushed forward toward pericenter. That is, the longitude of conjunction always experiences a kind of restoring force that drives it toward pericenter. Conjunction at pericenter is therefore a stable equilibrium point; the effect of the resonance is to reinforce this configuration, and an analogy to a simple spring system suggests that we might well expect bounded oscillations or librations to occur about this equilibrium point. These are in fact observed.

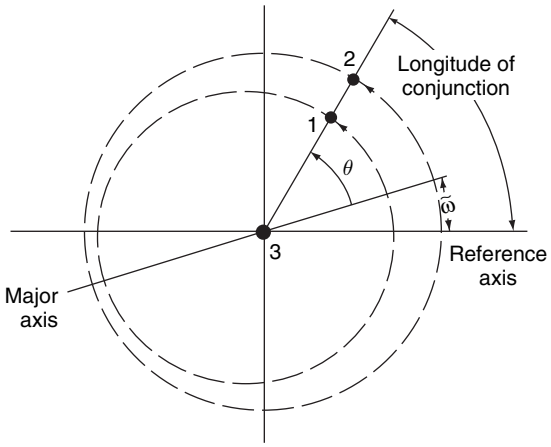

FIGURE 19.14 Satellites in conjunction. Since satellites 1 and 2 are moving away from pericenter, they will experience a kind of restoring force pushing the longitude of conjunction back towards pericenter. (From Greenberg, 1982).

Immediately prior and subsequent to conjunction, in addition to $\mathbf{F}_r$ acting outward, s_1 also experiences a tangential force component $\mathbf{F}_T$. $\mathbf{F}_T$ immediately before conjunction occurs while s_1 is overtaking s_2, so acts in the direction of s_1's motion in its orbit, whereas $\mathbf{F}_T$ immediately after conjunction occurs after s_1 has passed s_2, so acts in the opposite direction. However, for a conjunction after s_1 has passed ϖ_1, $\mathbf{F}_T$ immediately before conjunction is smaller than $\mathbf{F}_T$ immediately after, because the orbits are converging and the gravitational force increases as distance decreases. The net effect of these forces therefore sums to increase the orbital angular momentum H of s_1. By Eq. (19.6), with both a_1 and H changing, it is clear that s_1's eccentricity e_1 must in general also change.

These physical arguments can be put onto a mathematical footing by writing expressions for changes in specific energy E and angular momentum H due to a perturbing force $\mathbf{F}$ (Burns, 1976). $\dot{E}$ here is the work done per unit mass on a body per unit time by a disturbing force, so by the definition of work,

$$\dot{E} = \mathbf{F} \bullet \mathrm{d}\mathbf{r}/\mathrm{d}t = (\mathrm{d}r/\mathrm{d}t)F_r + r(\mathrm{d}\theta/\mathrm{d}t)\ F_T\ , \quad (19.9)$$

where F_r and F_T are the magnitudes of $\mathbf{F}_r$ and $\mathbf{F}_T$ and r and θ are the instantaneous radius and true longitude, respectively, of the orbit (defined in Fig. 19.3). Similarly, the time rate of change of H is just

$$\dot{\mathrm{H}} = |\mathbf{r} \times \mathbf{F}| = rF_r. \quad (19.10)$$

The normal force N does not appear in either Eq. (19.9) or (19.10) since we assume coplanar orbits. Differentiating Eq. (19.7), then using (19.9) provides an equation for da/dt in terms of a, e, F_r and F_T; similarly Eqs. (19.6), (19.9), and (19.10) provide an expression for de/dt. Analogous perturbation equations are derivable for the other orbital elements (Burns, 1976); in particular $d\varpi/dt = \dot{\varpi}_1$ also depends on a, e, F_r and F_T. In fact, one finds $\dot{\varpi}_1 \propto e^{-1}$. Therefore ϖ also varies due to orbit–orbit perturbations. Because of the resonance, these effects are reinforced over successive orbits.

Because the orbital longitude λ_1 of s_1 is measured with respect to ϖ_1, which itself is changing, the resonance condition $n_1 = j(n_1 - n_2)$ must be appropriately modified. If ϖ_1 shifts, then λ_1 shifts to $\lambda_1 - \varpi_1$. But since

$$\lambda_1 = \int n_1 dt\,, \tag{19.11}$$

n_1 shifts to κ_1, where $\kappa_1 \equiv n_1 - \dot{\varpi}_1$. κ_1 is simply the natural frequency of s_1 taking into account that the orbit itself is precessing at $\dot{\varpi}_1$. The condition for resonance therefore becomes $\kappa_1 = j(n_1 - n_2)$, or

$$jn_2 - (j-1)n_1 - \dot{\varpi}_1 = 0. \tag{19.12}$$

Equation (19.12) shows that observed resonances in the Solar System will not have exact whole number ratios between satellite periods or mean motions; these ratios will deviate slightly from whole number ratios due to the presence of small terms like $\dot{\varpi}_1$.

Finally, as previously noted, $\dot{\varpi}_1 \propto e^{-1}$, so that in order for $\dot{\varpi}_1$ to satisfy Eq. (19.12), e_1 must have a specific value. This eccentricity is the forced eccentricity that is set and maintained by the orbit–orbit resonance. (The importance of this forced eccentricity for the Galilean satellites was overlooked for many years, with the result that tidal heating went unpredicted; see Greenberg (1982) for a discussion.)

Laplace three-body resonance

The only known *three-body* resonance in the Solar System is the Laplace resonance among Io, Europa, and Ganymede. Adopting notation analogous to that used in our discussion of the two-body case, and as shown in Fig. 19.4, Io, Europa, and Ganymede are involved in a resonance where the mean motions satisfy

$$n_1 - 3n_2 + 2n_3 = 0\,. \tag{19.13}$$

This relationship among the three satellite mean motions, unlike that in Eq. (19.12), is strictly equal to zero (Murray and Dermott, 2001), with precision measured to eleven significant figures! The stability of the three-body Laplace resonance can only be sustained if the precessions of the satellites' orbits are equal. Expressing this mathematically, subtracting Eqs. (19.12) for the two satellite pairs, Eq. (19.13) follows only if $\dot{\varpi}_1 = \dot{\varpi}_2$.

Equation (19.13) corresponds by Eq. (19.11) to a relation among the satellites' orbital longitudes: $\lambda_1 - 3\lambda_2 + 2\lambda_3 = \phi \approx 180^\circ$. The approximation sign is a reminder that ϕ librates about 180°, with an amplitude of 0.064° and a period of 2071 days (Murray and Dermott, 2001). The fact that $\phi \approx 180^\circ$ guarantees that no triple conjunction of the three satellites ever takes place, as shown in Fig. 19.4. For example, whenever Europa and Ganymede are in conjunction ($\lambda_2 = \lambda_3$), Io must be 180° away, i.e., $\lambda_1 = \lambda_2 + 180^\circ$.

How did something as marvelous as the Laplace resonance arise? In one theory (Yoder, 1979), the Laplace resonance was assembled from an originally non-resonant configuration of the satellites' orbits by the differential expansion of the orbits due to tides raised on Jupiter by the satellites. To understand this effect, recall the discussion in Appendix (19.1). Equation (19.4) is the torque experienced by the tidal bulge raised on the satellite due to the primary. An analogous expression can be derived for the torque experienced by the primary, due to a tidal bulge raised on it by the gravity of the satellite. This expression is identical to Eq. (19.4), except with the substitutions $m_e \leftrightarrow M_J$, $r_e \leftrightarrow R_J$, and $k_2 \sin 2\varepsilon = k_2 Q$ now refers to the primary rather than the satellite. This torque acts to despin the primary (without much effect in the case, say, of Io and Jupiter), but by action–reaction, the torque slowing the planet acts as well on the satellite's orbit – which expands in response. (In the Earth–Moon system this expansion is thought to have driven the Moon from its formation near Earth out to its present distance of 60 Earth radii.)

We derive an equation for this tidally-driven orbital expansion for the special case where the orbit is circular and has zero inclination. (For the more general case, see Chyba *et al.*, 1989). The torque Γ and angular momentum H are related by

$$\Gamma = \dot{H}\,, \tag{19.14}$$

where Γ is given by Eq. (19.4) with the substitutions just described and H is from Eq. (19.6) with $e = 0$. Integrating the resulting equation for $\dot{a}$ gives

$$a^{13/2} = a_0^{13/2} + (13/2)\beta(t - t_0) \tag{19.15}$$

for the semimajor axis of the satellite's orbit as a function of time, measured with respect to initial time t_0 and semimajor axis a_0. Here $\beta = (39/2)(k_2/Q)_J m_e R_J^5 (G/M_J)^{1/2}$, and $(k_2/Q)_J$ refers to the primary. From Eq. (19.15), the timescale for orbital expansion $\tau \propto (a^{13/2} - a_0^{13/2})$; that is, satellites evolve outwards more quickly when they are closer to the primary. In the distant past Io's orbit therefore expanded more rapidly than Europa's, caught up to Europa, and drove it into the configuration where $n_1/n_2 \approx 2{:}1$. The two satellites were then captured into this stable resonance so that as Io's orbit continued to expand due to angular momentum exchange with Jupiter, Io transferred to Europa part of its increased angular momentum. In a similar way, the three-body lock of Io–Europa and Ganymede was subsequently established as the orbits of Io and Europa expanded and a 2:1 commensurability between the mean motions of Europa and Ganymede was approached. There has not been sufficient time since Solar System formation for Callisto to have been brought into the resonance.

This scenario, while elegant, requires Jupiter's Q_J to be $\sim 10^5$ –10^6 or smaller for sufficient expansion of the orbits to have occurred (Goldreich and Soter, 1966), and as low as $\sim 10^4$ to maintain the current configuration in equilibrium (Peale and Lee, 2002). An alternative, primordial origin for the Laplace relation has been proposed out of concern that these values for Q_J may be unreasonably small (Greenberg, 1982). This model involves differential migration of the newly formed Galilean satellites due to their interactions with the circumjovian accretion disk (Peale and Lee, 2002).

Appendix 19.5 Gravity and interior models

The gravitational potential for a non-spherical body may be expanded as an infinite series of spherical harmonics (Kaula, 1966). An approximation through second degree and order is:

$$V = \frac{Gm_e}{r}\left[1 - \frac{1}{2}J_2\left(\frac{r_e}{r}\right)^2(3\sin^2\phi - 1) + 3C_{22}\left(\frac{r_e}{r}\right)^2\cos^2\phi\cos 2\lambda\right], \quad (19.16)$$

where the coefficients J_2 and C_{22} measure the contributions to the gravitational potential of the spherical harmonics of degree l and order m for $l = 2$, $m = 0$ and $l = 2$, $m = 2$, respectively. The spherical coordinates are fixed in Europa (radius r, latitude ϕ, longitude λ), with longitude measured from the Europa–Jupiter line. The first term is the gravitational potential for a spherical body. J_2 arises from Europa's oblateness due to its rotation about its spin axis. Longitude-dependent C_{22} is required by the asymmetry (about its rotation axis) in Europa's permanent tidal bulge.

Both J_2 and C_{22} are directly related to Europa's internal mass distribution. $J_2 \approx (C - A/m)_e r_e^2$ and $C_{22} \approx (B - A)/4m_e r_e^2$, where C is Europa's axial moment of inertia and A and B are its equatorial moments. For a body in rotational and tidal equilibrium, C_{22} is related to the "rotational response" parameter $q = \omega^2 r_e^3/Gm_e$ (the ratio of centrifugal to gravitational acceleration at Europa's equator), where ω is the satellite's rotational angular velocity. In fact,

$$C_{22} = 3\alpha q/4, \quad (19.17)$$

where α is a dimensionless coefficient that depends on the distribution of mass within the satellite. With q known and C_{22} obtained from spacecraft Doppler measurements, α may be determined by Eq. (19.17); Anderson *et al.* (1998) have measured $\alpha = 0.35$. The satellite's axial moment of inertia C then follows from the relationship (Anderson *et al.*, 1996):

$$\frac{C}{m_e r_e^2} = \frac{2}{3}\left[1 - \frac{2}{5}\left(\frac{4 - 3\alpha}{1 + 3\alpha}\right)^{1/2}\right]. \quad (19.18)$$

For Europa $C/m_e r_e^2 = 0.346 \pm 0.005$, which is less than 0.4, the value for a sphere of constant density, implying that Europa must have a concentration of mass towards its center. Europa's mean density and C then in turn provide constraints on two- or three-layer models for the internal mass distribution (Anderson *et al.*, 1998).

Appendix 19.6 Induced magnetic fields

Jupiter's magnetic field axis is anchored in the planet, tilted by 9.6° from its spin axis and offset by 0.13 R_J from its center (NSSDC, 2004). Therefore, over one jovian rotational period (synodic period of 11.23 hr, i.e., as experienced by Europa), Europa experiences a periodic time-varying magnetic field. Consider a projection of Jupiter's magnetic field on to Jupiter's equatorial plane. At Europa this can be resolved into two components, $\mathbf{B}_1$ in the x-direction (the radial direction, pointing toward Jupiter) and $\mathbf{B}_2$ in the y-direction (the tangential direction of Europa's motion in its orbit). $\mathbf{B}_1$, for example, varies sinusoidally with a synodic period of 11.23 hours. By Faraday's law of electromagnetic induction, $\mathbf{B}_1$ induces an electric field given by $\nabla \times \mathbf{E} = -\partial \mathbf{B}_1/\partial t$, which in turn causes a

current I_1 to flow within Europa's conducting ocean. This eddy current I_1 (which changes direction twice each synodic period) encircles $\mathbf{B}_1$, setting up a secondary magnetic field of its own whose orientation is approximately antiparallel to the primary field, and which opposes the change in magnetic flux (Lenz's law). The Galileo spacecraft magnetometer indeed measured changes in the total magnetic field consistent with the presence of a secondary field whose direction changed in response to Jupiter's primary field (Kivelson *et al.*, 2000).

A primary magnetic field (from Jupiter) oscillating at frequency ω along a direction with unit vector $\mathbf{e}$ may be written $\mathbf{B}_p = B_p e^{-i\omega t}\mathbf{e}$. The total time-varying field is the sum of $\mathbf{B}_p$ and the secondary (induced) field $\mathbf{B}_s$. For a simple shell model of Europa, where a spherical conducting shell of conductivity σ is enclosed by an insulating core and insulating outer shell, the solution to the induced field at a vector distance $\mathbf{r}$ outside the conducting shell is $\mathbf{B}_p + \mathbf{B}_s$, where

$$\mathbf{B}_s = -Ae^{-i(\omega t+\phi)} B_p[3(\mathbf{r} \bullet \mathbf{e})\mathbf{r} - r^2\mathbf{e}]r_e^2/2r^5, \quad (19.19)$$

which is a dipole field. Here A and ϕ are real numbers that depend on the thickness of the conducting layer within Europa and the conductivity of that layer. Comparing this simple shell model to Galileo observations suggests that Europa's internal conductor must have a conductivity exceeding $0.06\,\mathrm{S\,m^{-1}}$ at a depth of less than 200 km below the surface (Zimmer *et al.*, 2000).

Appendix 19.7 Heat conduction and convection

We explain here how the subsurface conductive temperature gradients shown in Fig. 19.12 result from solutions of the one-dimensional time-independent thermal diffusion equation, given different assumptions about the nature of tidal heating. We then explain the origin of the Rayleigh number and show why it provides a criterion for whether heat loss will occur primarily through conduction or convection.

Conduction

Consider heat flow through Europa's ice shell in a coordinate system where z measures the depth into the ice below the surface. Fourier's empirical law says that the heat flux H (erg $\mathrm{s^{-1}\,cm^{-2}}$) is directly proportional to the temperature gradient $\partial T/\partial z$:

$$H = k\ \partial T/\partial z\,.^{17} \quad (19.20)$$

The thermal conductivity k of ice is given by

$$k(T) = a/T + b, \quad (19.21)$$

where $a = 4.88 \times 10^7$ erg $\mathrm{cm^{-1}\ s^{-1}}$ and $b = 4.68 \times 10^4$ erg $\mathrm{cm^{-1}\ s^{-1}\ K^{-1}}$ (Hobbs, 1974). For mathematical tractability in analytical work, $k(T)$ is often taken either to be a constant and assigned its value at some median temperature (say 185 K), or b is set to zero, a good approximation for temperatures below $\sim 10^3$ K.

The rate at which a unit volume in a given subsurface layer heats up is due to the volumetric tidal heating rate within that layer, q (erg $\mathrm{cm^{-3}\ s^{-1}}$), and the difference between heat flows H in and out. For an infinitesimal layer, this becomes

$$q + \partial H/\partial z = \rho C_P\ \partial T/\partial t, \quad (19.22)$$

where ρ is the density of the material and C_P is the specific heat capacity at constant pressure (the amount of heat needed to raise the temperature of one gram of ice by 1 K at constant pressure). Both C_P and ρ for ice are temperature-dependent (Hobbs, 1974).

Combining Eqs. (19.20) and (19.22) yields the thermal diffusion equation

$$q + \partial(k\partial T/\partial z)/\partial z = \rho C_P\,\partial T/\partial t. \quad (19.23)$$

We want the time-independent equation, for which $\partial T/\partial t = 0$:

$$\partial(k\partial T/\partial z)/\partial z = -q. \quad (19.24)$$

Solutions of Eq. (19.24) give steady-state temperature gradients in Europa's ice; Eq. (19.23) is required for cases where melting (O'Brien *et al.*, 2002) or refreezing (Buck *et al.*, 2002) is being modeled.

Were k constant and $q \approx 0$, Eq. (19.20) gives the thickness of the ice layer as

$$h = k\Delta T/H, \quad (19.25)$$

where $\Delta T = T_h - T_s$ and T_s and T_h are the temperatures at the surface and base of the ice layer, respectively. In this case Eq. (19.24) yields a simple linear temperature profile through the ice,

$$T(z) = T_s + z\Delta T/h. \quad (19.26)$$

[17] The right-hand side of Eq. (19.20) is positive, which is opposite to the usual sign convention for Fourier's law, because of our choice of z increasing downward into the ice shell.

However, q is positive in Europa's ice due to tidal heating in the shell; if its value is taken to be constant throughout the shell, Eq. (19.24) gives

$$T(z) = T_s \exp[(H + qh)z/a - qz^2/2a]. \quad (19.27)$$

But for realistic ice rheologies, q is extremely temperature dependent and the assumption of constant q is poor. For example, $q \propto \exp[l(1 - T_m/T)]$, where T_m is the melting temperature and $l \approx 24$ at T_m (Ojakangas and Stevenson, 1989). In this case, tidal heating is confined to the warmest ice, i.e., to a thin layer at the base of the ice shell. Equation (19.24) can be solved for the case where q is strongly peaked in warm ice; one finds (Chyba *et al*., 1998)

$$T(z) = T_s \exp[(z/h)\ln(T_h/T_s)]. \quad (19.28)$$

Plotted in Fig. 19.12 are the temperature gradients, corresponding to Eqs. (19.26) to (19.28), assuming the same ice layer thickness in each case. Equation (19.28) is most likely the best approximation for Europa, assuming that the shell loses heat primarily through conduction rather than convection, and is thick enough for tidal heating to be important.

Convection

Will Europa's ice lose heat primarily through conduction or convection? The usual criterion to answer this question is the value of the *Rayleigh number Ra* (Rayleigh, 1916). The Rayleigh number that is usually cited in the Europa literature as determining the onset of convection (e.g., Pappalardo *et al*., 1998; McKinnon, 1999) is:

$$Ra = \rho g \alpha_V \Delta T h_c^3/\eta\kappa, \quad (19.29)$$

where g is the surface gravity, α_V the volumetric coefficient of thermal expansion, η the dynamic viscosity, $\kappa = k/\rho C_P$ is the thermal diffusivity, and h_c is the thickness of the ice beneath the stagnant lid. Convection will occur when Ra exceeds some critical value Ra_{crit}, usually taken to be $\sim 10^3$; Since $Ra \propto h_c{}^3$, there is a critical thickness h_c above which convection occurs.

This expression for Ra is derived by applying linear stability analysis to a set of four differential equations describing thermal convection for a particular system, but these assume that k is constant and $q = 0$ in Eq. (19.23). Given the importance of tidal heating within Europa's ice shell, it is not obvious why investigators have chosen this formulation for Ra. For example, a Rayleigh number appropriate for a layer heated uniformly from within is (Turcotte and Schubert, 1982):

$$Ra = \rho^2 g \alpha_V q h_c^5/k\eta\kappa. \quad (19.30)$$

Ra_{crit} for Eq. (19.30) is again $\sim 10^3$. The difference between Eqs. (19.29) and (19.30) should lead to caution in evaluating conclusions based solely on Eq. (19.29). An additional uncertainty concerns the observation that η depends not only on temperature but also on other properties such as the grain size of the ice.

References

Anderson, J. D., Sjogren, W. L., and Schubert, G. (1996). Galileo gravity results and the internal structure of Io. *Science*, **272**, 709–712.

Anderson, J. D., Lau, E. L., Sjogren, W. L. *et al*. (1998). Europa's differentiated internal structure: inferences from four Galileo encounters. *Science*, **281**, 2019–2022.

Auda, H. and Emborg, C. (1973). Studies on post-irradation degradation in *Micrococcus radiodurans*, strain $R_{11}5$. *Radiation Research*, **53**, 273–280.

Bada, J. L., Bigham, C., and Miller, S. L. (1994). Impact melting of frozen oceans on the early Earth: implications for the origin of life. *Proc. Natl. Acad. Sci. USA*, **91**, 1248–1250.

Bada, J. L. and Lazcano, A. (2002). Some like it hot, but not the first biomolecules. *Science*, **296**, 1982–1983.

Barr, A. C. and Pappalardo, R. T. (2003). Numerical simulations of non-Newtonian convection in ice: application to Europa. *Lunar Planet. Sci.* **XXXIV**, abs. 1477. Houston, TX: Lunar and Planetary Institute [CD-ROM].

Buck, L., Chyba, C. F., Goulet, M., Smith, A., and Thomas, P. (2002). Persistence of thin ice regions in Europa's ice crust. *Geophys. Res. Lett*., **29**, 2055, doi:10.1029/2002GL016171.

Burns, J. A. (1976). Elementary derivation of the perturbation equations of celestial mechanics. *Am. J. Phys*., **44**, 944–949 (Erratum: **45**, 1230).

Carlson, R. W., Johnson, R. E., and Anderson, M. S. (1999a). Sulfuric acid on Europa and the radiolytic sulfur cycle. *Science*, **286**, 97–99.

Cassen, P., Peale, S. J., and Reynolds, R. T. (1982). Structure and thermal evolution of the Galilean satellites. In *Satellites of Jupiter*, ed. D. Morrison, pp. 93–128. Tucson: University of Arizona Press.

Chapelle, F. H., O'Neill, K., Bradley, P. M. *et al*. (2002). A hydrogen-based subsurface microbial community dominated by methanogens. *Nature*, **415**, 312–314.

Chyba, C. F. and Hand, K. P. (2001). Life without photosynthesis. *Science*, **292**, 2026–2027.

Chyba, C. F. and McDonald, G. D. (1995). The origins of life in the solar system: current issues. *Ann. Rev. Earth Planet. Sci*., **23**, 215–249.

Chyba, C. F. and Phillips, C. B. (2001). Possible ecosystems and the search for life on Europa. *Proc. Natl. Acad. Sci. USA*, **98**, 801–804.

Chyba, C. F. and Phillips, C. B. (2002). Europa as an abode of life. *Orig. Life Evol. Biosphere*, **32**, 47–68.

Chyba, C. F. and Sagan, C. (1987). Infrared emission by organic grains in the coma of comet Halley. *Nature*, **330**, 350–353.

Chyba, C. F., Jankowski, D. G., and Nicholson, P. D. (1989). Tidal evolution in the Neptune–Triton system. *Astron. Astrophys.*, **219**, L23–L26.

Chyba, C. F., Ostro, S. J., and Edwards, B. C. (1998). Radar detectability of a subsurface ocean on Europa. *Icarus*, **134**, 292–302.

Colburn, D. S. and Reynolds, R. T. (1985). Electrolytic currents in Europa. *Icarus*, **63**, 39–44.

Cooper, J. F., Johnson, R. E., Mauk, B. H., Garrett, H. B., and Gehrels, N. (2001). Energetic ion and electron irradiation of the icy Galilean satellites. *Icarus*, **149**, 133–159.

Cooper, J. F., Phillips, C. B., Green, J. R. *et al.* (2002). Europa exploration: science and mission priorities. In *The Future of Solar System Exploration, 2003–2013*, ed. M. Sykes, pp. 217–252. San Francisco: Astronomical Society of the Pacific.

Dalton, J. B., Mogul, R., Kagawa, H. K. *et al.* (2003). Near-infrared detection of potential evidence for microscopic organisms on Europa. *Astrobiology*, **3**, 505–529.

Delitsky, M. L. and Lane, A. L. (1998). Ice chemistry on the Galilean satellites. *J. Geophys. Res.*, **103**, 31,391–31,403.

Fagents, S. A., Greeley, R., Sullivan, R. J. *et al.* (2000). Cryomagmatic mechanisms for the formation of Rhadamanthys Linea, triple band margins, and other low-albedo features on Europa. *Icarus*, **144**, 54–88.

Figueredo, P. H., Chuang, F. C., Rathbun, J. *et al.* (2002). Geology and origin of Europa's "Mitten" feature (Murias Chaos). *J. Geophys. Res.*, **107(E5)**, 5026, doi:10.1029/2001JE001591.

Gaidos, E. J. and Nimmo, F. (2000). Tectonics and water on Europa. *Nature*, **405**, 637.

Gaidos, E. J., Nealson, K. H., and Kirschvink, J. L. (1999). Life in ice-covered oceans. *Science*, **284**, 1631–1633.

Galileo, G. (1610). *Sidereus Nuncius, or, The Sidereal Messenger* (trans. and intro. by A. van Helden). Chicago: University of Chicago Press (1989).

Geissler, P. E. (2000). Cryovolcanism in the outer solar system. In *Encyclopedia of Volcanoes*, ed. H. Sigurdsson, pp. 785–800. San Diego, CA: Academic.

Geissler, P. E., Greenberg, R., Hoppa, G. *et al.* (1998). Evidence for non-synchronous rotation of Europa. *Nature*, **391**, 368.

Goldreich, P. (1966). Final spin states of planets and satellites. *Astron. J.*, **71**, 1–7.

Goldreich, P. and Soter, S. (1966). Q in the Solar System. *Icarus*, **5**, 375–389.

Greeley, R., Figueredo, P. H., Williams, D. A. *et al.* (2000). Geologic mapping of Europa. *J. Geophys. Res.*, **105**, 22559–22578.

Greeley, R., Chyba, C. F., Head, J. W. *et al.* (2004). Geology of Europa. In *Jupiter: the Planets, Satellites and Magnetosphere*, eds. F. Bagnold, T. E. Dowling, W. B. McKinnon, *et al.* Cambridge: Cambridge University Press.

Greenberg, R. (1982). Orbital evolution of the Galilean satellites. In *Satellites of Jupiter*, ed. D. Morrison, pp. 65–92. Tucson: University of Arizona Press.

Greenberg, R. and Weidenschilling, S. J. (1984). How fast do Galilean satellites spin? *Icarus*, **58**, 186–196.

Greenberg, R., Geissler, P., Hoppa, G. *et al.* (1998). Tectonic processes on Europa: tidal stresses, mechanical response, and visible features. *Icarus*, **135**, 64–78.

Greenberg, R., Hoppa, G. V., Tufts, B. R., Geissler, P. E., and Reilly, J. (1999). Chaos on Europa. *Icarus*, **141**, 263–286.

Greenberg, R., Geissler, P., Tufts, B. R., and Hoppa, G. V. (2000). Habitability of Europa's crust: the role of tidal-tectonic processes. *J. Geophys. Res.*, **105**, 17,551–17,562.

Guillot, T. (1999). A comparison of the interiors of Jupiter and Saturn. *Planet. Space Sci.*, **47**, 1183–1200.

Hand, K. H. and Chyba, C. F. (2007). Empirical constraints on the salinity of the europan ocean and implications for a thin ice shell. *Icarus*, in press.

Head, J. W. III and Pappalardo, R. T. (1999). Brine mobilization during lithospheric heating on Europa: implications for formation of chaos terrain, lenticula texture, and color variations. *J. Geophys. Res.*, **104**, 27,143.

Head, J., Pappalardo, R. T., and Sullivan, R. J. (1999). Europa: morphological characteristics of ridges and triple bands from Galileo data (E4 and E6) and assessment of a linear diapirism model. *Geophys. Res. Lett.*, **104**, 24,223–24,236.

Hobbs, P. V. (1974). *Ice Physics*. Oxford: Oxford University Press.

Hoppa, G., Tufts, B. R., Greenberg, R., and Geissler, P. (1999a). Strike-slip faults on Europa: global shear patterns driven by tidal stress. *Icarus*, **141**, 287–298.

Hoppa, G. V., Tufts, B. R., Greenberg, R., and Geissler, P. (1999b). Formation of cycloidal features on Europa. *Science*, **285**, 1899–1902.

Hoppa, G. V., Greenberg, R., Tufts, B. R. *et al.* (1999c). Rotation of Europa: constraints from terminator and limb positions. *Icarus*, **137**, 341–347.

Horneck, G. (1993). Responses of *Bacillus subtilis* spores to space environment: results from experiments in space. *Origins Life Evol. Biosphere*, **23**, 37–52.

Hoyle, F. and Wickramasinghe, N. C. (1987). Organic dust in comet Halley. *Nature*, **328**, 117.

Hussmann, H. and Spohn, T. (2004). Thermal-orbital evolution of Io and Europa. *Icarus*, **171**, 391–410.

Ip, W.-H. (1996). Europa's oxygen exosphere and its magnetospheric interaction. *Icarus*, **120**, 317–325.

Johnson, R. E. (1998). Sputtering and desorption from icy surfaces. In *Solar System Ices*, ed. B. Schmitt, C. de Bergh, and M. Festou, pp. 303–334. Dordrecht, The Netherlands: Kluwer.

Kanavarioti, A., Monnard, P., and Deamer, D. W. (2001). Eutectic phases in ice facilitate nonenzymatic nucleic acid synthesis. *Astrobiology*, **1**, 271–281.

Kargel, J. S., Kage, J. Z., Head, J. W. *et al.* (2000). Europa's crust and ocean: origin, composition, and the prospects for life. *Icarus*, **148**, 226–265.

Kattenhorn, S. A. (2002). Nonsynchronous rotation evidence and fracture history in the bright plains region, Europa. *Icarus*, **157**, 490–506.

Kaula, W. M. (1966). *Theory of Satellite Geodesy*. New York: Dover.

Kivelson, M. G., Khurana, K. K., Russell, C. T., Volwerk, M., Walker, R. J., and Zimmer, C. (2000). Galileo magnetometer measurements: a stronger case for a subsurface ocean at Europa. *Science*, **289**, 1340–1343.

Kivelson, M. G., Khurana, K. K., and Volwerk, M. (2002). The permanent and inductive magnetic moments of Ganymede. *Icarus*, **157**, 507–522.

Kovach, R. L. and Chyba, C. F. (2001). Seismic detectability of a subsurface ocean on Europa. *Icarus*, **150**, 279–287.

Kuramoto, K. and Matsui, T. (1994). Formation of a hot proto-atmosphere on the accreting giant icy satellite: implications for the origin and evolution of Titan, Ganymede, and Callisto. *J. Geophys. Res.*, **99**, 21183–21200.

Levy, M., Miller, S. L., Brinton, K., and Bada, J. L. (2000). Prebiotic synthesis of adenine and amino acids under Europa-like conditions. *Icarus*, **145**, 609–613.

MacDonald, G. J. F. (1964). Circulation and tides in the high atmosphere. *Planet. Space Sci.*, **10**, 79–87.

McCollom, T. M. (1999). Methanogenesis as a potential source of chemical energy for primary biomass production by autotrophic organisms in hydrothermal systems on Europa. *J. Geophys. Res.*, **104**, 30,729–30,742.

McCord, T. B., Hansen, G. B., Clark, R. N. *et al.* (1998). Non-water-ice constituents in the surface material of the icy Galilean satellites from the Galileo near-infrared mapping spectrometer investigation. *J. Geophys. Res.*, **103**, 8603–8626.

McCord, T. B., Hansen, G. B., Matson, D. L. *et al.* (1999). Hydrated salt minerals on Europa's surface from the Galileo near-infrared mapping spectrometer (NIMS) investigation. *J. Geophys. Res.*, **104**, 11,827–11,851.

McKinnon, W. B. (1999). Convective instability in Europa's floating ice shell. *Geophys. Res. Lett.*, **26**, 951–954.

McKinnon, W. B. and Shock, E. L. (2001). Ocean Karma: what goes around comes around on Europa (or does it?). *Lunar Planet. Sci.*, **XXXII**, Abs. #2181. Houston, TX: Lunar and Planetary Institute.

McKinnon, W. B. and Zolensky, M. E. (2003). Sulfate content of Europa's ocean and shell: evolutionary considerations and some geological and astrobiological implications. *Astrobiology*, **3**, 879–897.

Monnard, P., Apel, C., Kanavarioti, A., and Deamer, D. (2002). Influence of ionic inorganic solutes on self-assembly and polymerization processes related to early forms of life: implications for a prebiotic aqueous medium. *Astrobiology*, **2**, 139.

Moore, J. C. (2000). Models of radar absorption in europan ice. *Icarus*, **147**, 292–300.

Moore, J. M., Asphaug, E., Sullivan, R. J. *et al.* (1998). Large impact features on Europa: results of the Galileo nominal mission. *Icarus*, **135**, 127–145.

Moore, J. M., Asphaug, E. Belton, M. J. S. *et al.* (2001). Impact features on Europa: results of the Galileo Europa mission (GEM). *Icarus*, **151**, 93–111.

Moore, W. B. and Schubert, G. (2000). The tidal response of Europa. *Icarus*, **147**, 317–319.

Mumma, M. J., Weissman, P. R., and Stern, S. A. (1993). Comets and the origin of the Solar System: reading the Rosetta Stone. In *Protostars and Planets III*, ed. E. H. Levy and J. I. Lunine, pp. 1177–1252. Tucson: University of Arizona Press.

Murray, C. D. and Dermott S. F. (2001). *Solar System Dynamics*. Cambridge: Cambridge University Press.

National Space Science Data Center (2004). Planetary Fact Sheets. nssdc.gsfc.nasa.gov/planetary/planetfact.html. Visited 11/17/2004.

Newton, I. (1686). *Philosophiae Naturalis Principia Mathematica*. In *Sir Isaac Newton's Mathematical Principles of Natural Philosophy and his System of the World*, ed. F. Cajori. Berkeley: University of California Press (1934).

O'Brien, D. P., Geissler, P., and Greenburg, R. (2002). A melt-through model for chaos formation on Europa. *Icarus*, **156**, 152–161.

Ojakangas, G. W. and Stevenson, D. J. (1989). Thermal state of an ice shell on Europa. *Icarus*, **81**, 220–241.

Pappalardo, R. T., Head, J. W., Greeley, R. *et al.* (1998). Geological evidence for solid-state convection in Europa's ice shell. *Nature*, **391**, 365–368.

Pappalardo, R. T., Belton, M. J. S., Brereman, H. H. *et al.* (1999). Does Europa have a subsurface ocean? Evaluation of the geological evidence. *J. Geophys. Res.*, **104**, 24,015–24,055.

Peale, S. J. and Cassen, P. (1978). Contribution of tidal dissipation to lunar thermal history. *Icarus*, **36**, 245–269.

Peale, S. J., Cassen, P., and Reynolds, R. T. (1979). Melting of Io by tidal dissipation. *Science*, **203**, 892–894.

Peale, S. J. and Lee, M. H. (2002). A primordial origin of the Laplace relation among the Galilean satellites. *Science*, **298**, 593–597.

Phillips, C. B., McEwen, A. S., Hoppa, G. V. *et al*. (2000). The search for current geologic activity on Europa. *J. Geophys. Res*., **105**, 22,579–22,597.

Pierazzo, E. and Chyba, C. F. (2002). Cometary delivery of biogenic elements to Europa. *Icarus*, **157**, 120–127.

Pollack, J. B. and Sagan, C. (1967). Secular changes and dark-area regeneration on Mars. *Icarus*, **6**, 434–439.

Prockter, L. M. and Pappalardo, R. T. (2000). Folds on Europa: implications for crustal cycling and accommodation of extension. *Science*, **289**, 941–944.

Prockter, L. M., Head, J. W. III, Pappalardo, R. T. *et al*. (2002). Morphology of Europan bands at high resolution: a mid-ocean ridge-type rift mechanism. *J. Geophys. Res*., **107**, 5028, doi:10.1029/2000JE001458.

Raleigh, L. (1916). On convection currents in a horizontal layer of fluid when the higher temperature is on the underside. *Phil. Mag. Ser*. 6, **32**, 529–546.

Reynolds, R. T., Squyres, S. W., Colburn, D. S., and McKay, C. P. (1983). On the habitability of Europa. *Icarus*, **56**, 246–254.

Sagan, C. (1996). Circumstellar habitable zones: an introduction. In *Circumstellar Habitable Zones*, ed. L. R. Doyle, pp. 3–14. Menlo Park, CA: Travis House.

Sagan, C. and Chyba, C. (1997). The early faint sun paradox: organic shielding of ultraviolet-labile greenhouse gases. *Science*, **276**, 1217–1221.

Sarid, A. R., Greenberg, R., Hoppa, G. V., Hurford, T. A., Tufts, B. R., and Geissler, P. (2002). Polar wander and surface convergence of Europa's ice shell: evidence from a survey of strike-slip displacement. *Icarus*, **158**, 24–41.

Schenk, P. M. (2002). Thickness constraints on the icy shells of the galilean satellites from a comparison of crater shapes. *Nature*, **417**, 419–421.

Schulze-Makuch, D. and Irwin, L. N. (2004). *Life in the universe. Expectations and constraints*. Berlin: Springer-Verlag.

Sotin, C., Head, J. W., and Tobie, G. (2002). Europa: tidal heating of upwelling thermal plumes and the origin of lenticulae and chaos melting. *Geophys. Res. Lett*., **29**, 74–1, 1233, doi:10.1029/2001GL013844.

Space Studies Board, National Research Council (1992). *Biological Contamination of Mars: Issues and Recommendations*. Washington DC: National Academy Press, www.nas.edu/ssb/bcmarsmenu.htm.

Space Studies Board, National Research Council (2000). *Preventing the Forward Contamination of Europa*. Washington DC: National Academy of Sciences Press, www.nas.edu/ssb/europamenu.htm.

Spaun, N. A., Head, J. W., Collins, G. C., Prockter, L. M., and Pappalardo, R. T. (1998). Conamara Chaos region, Europa: reconstruction of mobile polygonal ice blocks. *Geophys. Res. Lett*., **25**, 4277–4280.

Spencer, J. R., Tamppari, L. K., Martin, T. Z., and Travis, L. D. (1999). Temperatures on Europa from Galileo Photopolarimeter-Radiometer: nighttime thermal anomalies. *Science*, **284**, 1514–1516.

Squyres, S. W., Reynolds, R. T., Cassen, P. M., and Peale, S. J. (1983). Liquid water and active resurfacing on Europa. *Nature*, **301**, 225–226.

Squyres, S. W., Reynolds, R. T., and Lissauer, J. J. (1985). The enigma of the Uranian satellites' orbital eccentricities. *Icarus*, **61**, 218–223.

Stacey, F. D. (1977). *Physics of the Earth*, second edn. New York: Wiley.

Stevenson, D. J. (1982). Interiors of the giant planets. *Ann. Rev. Earth Planet. Sci*., **10**, 257–295.

Stevenson, D. J. (2000a). Europa's ocean – the case strengthens. *Science*, **289**, 1305–1307.

Stevenson, D. J. (2000b). Limits on the variation of thickness of Europa's ice shell. *Lunar Planet. Sci*., **XXXI**, Abs. #1506. Houston: Lunar and Planetary Institute.

Sullivan, R., Greeley, R., Homan, K. *et al*. (1998). Episodic plate separation and fracture infill on the surface of Europa. *Nature*, **391**, 371.

Thomas, P. J. and Schubert, G. (1986). Crater relaxation as a probe of Europa's interior. *J. Geophys. Res*., **91**, 453–459.

Thomson, R. E. and Delaney, J. R. (2001). Evidence for a weakly stratified Europan ocean sustained by seafloor heat flux. *J. Geophys. Res*., **106**, 12355–12366.

Tufts, B. R., Greenberg, R., Hoppa, G., and Geissler, P. (1999). Astypalaea Linea: a large-scale strike-slip fault on Europa. *Icarus*, **141**, 53–64.

Turcotte, D. L. and Schubert, G. (1982). *Geodynamics: Application of Continuum Physics to Geological Problems*. New York: John Wiley & Sons.

Turtle, E. P. and Pierazzo, E. (2001). Thickness of a Europan ice shell from impact crater simulations. *Science*, **294**, 1326–1328.

Warren, S., Brandt, R. E., Grenfell, T. C., and McKay, C. P. (2002). Snowball Earth: ice thickness on the tropical ocean. *J. Geophys. Res*., **107**, 31–1, 3167, doi:10.1029/2001JC001123.

Whitman, W. B., Coleman, D. C., and Wiebe, W. J. (1998). Prokaryotes: the unseen majority. *Proc. Natl. Acad. Sci. USA*, **95**, 6578–6583.

Williams, K. K., and Greeley, R. (1998). Estimates of ice thickness in the Conamara Chaos region of Europa. *Geophys. Res. Lett*., **25**, 4273–4276.

Yoder, C. F. (1979). How tidal heating in Io drives the Galilean orbital resonance locks. *Nature*, **279**, 767–770.

Zahnle, K., Dones, L., and Levison, H. F. (1998). Cratering rates on the Galilean Satellites. *Icarus*, **136**, 202–222.

Zimmer, C., Khurana, K., and Kivelson, M. G. (2000). Subsurface oceans on Europa and Callisto: constraints from Galileo magnetometer observations. *Icarus*, **147**, 329–347.

Zolotov, M. Y. and Shock, E. L. (2001). Composition and stability of salts on the surface of Europa and their oceanic origin. *J. Geophys. Res.*, **106**, 32815–32827.

Further Reading and Surfing

galileo.jpl.nasa.gov Galileo spacecraft website; for images and general information.

Achenbach, J. (1999). *Captured by Aliens: the Search for Life and Truth in a Very Large Universe*. New York: Simon and Schuster. Terrific romp through the search for extraterrestrial life, including at Europa.

Bagnold, F., ed. (2004). *Jupiter: the Planet, Satellites and Magnetosphere*. New York: Cambridge University Press. The most up-to-date summary of the Jupiter system, including a synthesis of Galileo spacecraft data. Graduate-level text.

Beatty, J. K., ed. (1999). *The New Solar System*, fourth edn. Cambridge, MA: Sky Publishing. Fabulous introduction to the Solar System, suitable for a general audience and for scientists.

Demy, M. W. (1993). *Air and Water: the Biology and Physics of Life's Media*. Princeton: Princeton University Press. Compilation of the physics relevant to water's role in biology.

Greenberg, R. (2005). *Europa, the Ocean Moon*. New York: Spinger-Verlag. Inside information on the Galileo mission, and a summary of scientific results for Europa.

Johnson, T. V. (2004). A look at the Galilean satellites after the Galileo mission. *Physics Today*, **57**, 77–83 (April). Nice overview for nonexpert scientists.

Lewis, J. S. (1995). *Physics and Chemistry of the Solar System*. San Diego: Academic Press. Solar System chemistry and physics.

Sagan, C. (1994). *Pale Blue Dot: a Vision of the Human Future in Space*. New York: Random House. Visionary work on planetary habitability and astrobiology.